Helsinki University of Technology Control Engineering

Espoo February 2010 Report 165

COMPUTATIONAL MODELS FOR MICROVIA FILL PROCESS CONTROL

Antti Pohjoranta

Doctoral dissertation for the degree of Doctor of Science in Techology to be presented with due permission of the Faculty of Electronics, Communications and Automation for public examination and debate in Auditorium AS2 at the Aalto University School of Science and Technology (Espoo, Finland) on the 19th of March 2010 at 12 noon.

Aalto University

School of Science and Technology

Faculty of Electronics, Communications and Automation

Department of Automation and Systems Technology

Distribution:
Aalto University
Department of Automation and Systems Technology
P.O. Box 15500
FI-00076 Aalto, Finland
Tel. +358-9-470 25201
Fax. +358-9-470 25208
E-mail: control.engineering@tkk.fi
http://autsys.tkk.fi/

ISBN 978-952-60-3063-0 (printed)
ISBN 978-952-60-3064-7 (pdf)
ISSN 0356-0872

URL: http://lib.tkk.fi/Diss/2010/isbn9789526030647

Yliopistopaino
Helsinki 2010

Aalto University

ABSTRACT OF DOCTORAL DISSERTATION	AALTO UNIVERSITY SCHOOL OF SCIENCE AND TECHNOLOGY P. O. BOX 11000, FI-00076 AALTO http://www.aalto.fi

Author Antti Pohjoranta

Name of the dissertation

Computational models for microvia fill process control

Manuscript submitted October 26, 2009	Manuscript revised February 3, 2010
Date of the defence March 19, 2010	
☐ Monograph	☒ Article dissertation (summary + original articles)

Faculty	Faculty of Electronics Telecommunication and Automation
Department	Department of Automation and Systems Technology
Field of research	Control Engineering
Opponent(s)	Dr. Jaan Kalda
Supervisor	Prof. Heikki Koivo
Instructor	Prof. Robert Tenno

Abstract

The microvia fill process is an electrochemical copper deposition process applied in the manufacturing of multilayered printed circuit boards (PCBs). It is the process where the metallic interconnections between adjacent signal layers of the multilayered PCB are made. The process chemistry is complex, including the interactions of several additive chemicals in addition to the underlying basic electrochemical processes of copper electrodeposition. To this day, the microvia fill process equipment set-ups utilized in the industry have none or very little automatic online control of the process variables. This is mostly because direct online measuring of the microvia fill process is practically impossible due to the vast number of microscopic features on a PCB, as well as to the small size of the features.

The electronics industry is continuously striving to produce cheaper, smaller and more complex devices for an immeasurable number of applications. In the core of every electronics-appliance there is a PCB, which forms the chassis for the electronic components of the device as well as the signal paths between the components. Considering the enormous size of the electronics industry, as well as the ubiquitous nature of electronics, it is clear why PCB manufacturers consider that improving the microvia fill process technology is a relevant object for development.

This doctoral thesis presents novel means for improving the microvia fill process through process simulation and model-based process design. The main results of the thesis are distributed parameter models, which together form the main components necessary for modeling a practical microvia fill electrolysis apparatus and designing a model-based control system for the process. Though the models are primarily based on physical and chemical first principles, the development work of all models presented in this thesis relies on experimental data that is gathered to parameterize and to validate the models.

The thesis consists of a summary and nine publications, which address the modeling of the microvia fill process, the computational methods necessary for these models and the modeling of copper electrolysis systems in general.

Keywords microvia fill modeling, copper electroplating, electroplating modeling, ALE method	
ISBN (printed) 978-952-60-3063-0	ISSN (printed) 0356-0872
ISBN (pdf) 978-952-60-3064-7	ISSN (pdf)
Language English	Number of pages 54+73
Publisher Aalto University School of Science and Technology, Dpt. Automation and Systems Technology	
Print distribution Aalto University School of Science and Technology, Dpt. Automation and Systems Technology	
☒ The dissertation can be read at http://lib.tkk.fi/Diss/2010/isbn9789526030647	

Aalto-yliopisto

VÄITÖSKIRJAN TIIVISTELMÄ	AALTO-YLIOPISTO TEKNILLINEN KORKEAKOULU PL 11000, 00076 AALTO http://www.aalto.fi

Tekijä Antti Pohjoranta

Väitöskirjan nimi

Laskennallisia malleja mikrovian kuparitäyttöpinnoitusprosessin ohjausta varten

Käsikirjoituksen päivämäärä 26.10.2009	Korjatun käsikirjoituksen päivämäärä 3.2.2010

Väitöstilaisuuden ajankohta 19.3.2010

☐ Monografia	☒ Yhdistelmäväitöskirja (yhteenveto + erillisartikkelit)

Tiedekunta	Elektroniikan, tietoliikenteen ja automaation tiedekunta
Laitos	Automaatio- ja systeemitekniikan laitos
Tutkimusala	Systeemitekniikka
Vastaväittäjä(t)	Tri. Jaan Kalda
Työn valvoja	Prof. Heikki Koivo
Työn ohjaaja	Prof. Robert Tenno

Tiivistelmä

Mikrovian kuparitäyttöpinnoitusprosessi (microvia fill -prosessi) on monikerrospiirilevyjen tuotannossa käytetty sähkökemiallinen metallisointiprosessi. Prosessissa valmistetaan monikerrospiirilevyn sisäiset, levyllä vierekkäin sijaitsevien johdinkerrosten väliset johtimet. Prosessin kemia sisältää kuparin sähkökemialliseen pelkistämiseen liittyvien kemiallisten reaktioiden lisäksi useiden elektrolyyttilisäaineiden keskinäiset kemialliset vuorovaikutukset. Teollisuudessa käytettävät microvia fill -prosessilaitteistot sisältävät automaattisia online-ohjaustoimintoja edelleen hyvin vähän tai eivät lainkaan. Pääsyynä tähän on, että mikrovian täyttöpinnoituksen etenemistä on hyvin hankala mitata reaaliaikaisesti; piirilevyllä olevien pinnoitettavien piirteiden lukumäärä on valtava ja ne ovat kooltaan mikroskooppisen pieniä.

Elektroniikkateollisuuden toimijat pyrkivät jatkuvasti kehittämään halvempia, pienempiä ja monimutkaisempia laitteita lukemattomia eri sovelluksia varten. Elektroniikkatuotteiden runkona on lähes poikkeuksetta piirilevy, joka muodostaa paitsi laitteeseen asennettavat elektroniset komponentit kantavan rakenteen myös johtimet komponenttien välistä tiedonsiirtoa varten. Elektroniikkateollisuus on valtava teollisuuden ala ja elektroniikkatuotteita on nykyään lähes kaikkialla, joten on ymmärrettävää miksi piirilevyteollisuus näkee mikrovian täyttöpinnoitusprosessin kehittämisen merkityksellisenä.

Tässä väitöskirjassa esitetään uusia keinoja mikrovian täyttöpinnoitusprosessin kehittämiseen prosessin simuloinnin ja mallipohjaisen prosessisuunnittelun avulla. Väitöstyön päätuloksia ovat hajautettujen parametrien mallit, jotka yhdessä muodostavat todellisen microvia fill -järjestelmän tietokonemallintamiseen sekä järjestelmän mallipohjaisen säädön suunnitteluun tarvittavat mallikomponentit. Valtaosa työstä pohjautuu fysikaalisiin ja kemiallisiin perusperiaatteisiin, mutta kaikkia esitettyjä malleja varten on aina kerätty myös kokeellista mittausdataa, joka toimii lähtökohtana mallien parametrien määrittämiselle ja jota vasten mallit validoidaan.

Tämä väitöskirja koostuu yhteenveto-osasta sekä yhdeksästä julkaisusta, jotka käsittelevät mikrovian kuparitäyttöpinnoitusprosessia, sen tietokonemallintamista sekä kuparielektrolyysiprosessien tietokonemallintamista yleisesti.

Asiasanat kuparitäyttöpinnoitus, via fill mallinnus, elektrolyysimallinnus, ALE menetelmä

ISBN (painettu) 978-952-60-3063-0	ISSN (painettu) 0356-0872
ISBN (pdf) 978-952-60-3064-7	ISSN (pdf)
Kieli Englanti	Sivumäärä 54+73

Julkaisija Aalto-yliopisto, Teknillinen korkeakoulu, Automaatio- ja systeemitekniikan laitos

Painetun väitöskirjan jakelu Aalto-yliopisto, Teknillinen korkeakoulu, Automaatio- ja systeemitekniikan laitos

☒ Luettavissa verkossa osoitteessa http://lib.tkk.fi/Diss/

Preface

I started my work at the Helsinki University of Technology (HUT/TKK), Control Engineering Laboratory in the summer of 2005. Looking back now I feel like having actually come a fair bit since then, and through a number of twists. In 2005 electronics manufacturing – the industrial framework of this thesis – was still a healthy field of trade in Finland too. Who would've guessed that in a few years that business would have completely moved to Asia? The pace of change in the electronics industry has simply been unpredictably rapid during the first decade of this millennium.

Coincidentally, change has been all but absent at our university too. The Control Engineering laboratory, where I started, no longer exists as it was abolished when faculties were re-introduced in TKK some years ago. Recently, the Helsinki University of Technology was merged into the newly established Aalto University as the School of Science and Technology, which now includes a Control Engineering group. Though outwards these changes may seem cosmetic, behind them are an array of reforms that affect the everyday research work also.

Despite all the daunting turbulence around, the atmosphere at the Control Engineering group remained calm and inspiring through-out the years. Needless to say, a stable working environment is vital for long-term research work and hadn't it been for the excellent bunch of people who form our group, I bet also this thesis would have been left unfinished. I am sincerely grateful to all the people in the group, for their support and inspiration. These people are a perfect example of how one can actually be focused and ambitious, and do a good job, without really making such a big number out of it. Working in the group taught me enormously of for example team-work, leadership and vision, which weren't really much but buzzwords to me before I experienced these attributes in action at the lab.

From start to finish, my work was instructed by **prof. Robert Tenno** and I want to thank him heartily for all the time and effort he put into me. Without Robert's patience and endurance we certainly wouldn't always have ended up in a constructive conclusion after all those heated-up discussions at the office. I am also in great gratitude to my supervisor **prof. Heikki Koivo**, who gave me this opportunity in the first place and then stood up for my work when decisions were made. An exceptional character as he is, Heikki also stands out from the lab crew as a perfect example of how one *should* make at least a small number out of one's work, if aiming to be relevant and successful.

Also several people outside the TKK campus were of invaluable support during

the work. I want to thank **Mrs. Tarja Rapala-Virtanen** and especially **Mr. Timo Närhi** (Meadville Aspocomp International Limited, formerly Aspocomp) for enabling several significant matters during the different phases of this research. The effort of **Dr. Peifeng Chen** (Shanghai Meadville Science and Technology) and **prof. Toomas Tenno** (University of Tartu) who pre-examined the thesis is also acknowledged with great gratitude.

The fundamental resource for my research – money – was obtained from several sources, the most important one being once again the Finnish tax-payer's wallet, with The Finnish Funding Agency for Technology and Innovation (TEKES) and the Graduate School in Electronics, Telecommunication and Automation (GETA) being indispensable as mediators. Additional financial support was given by the Emil Aaltonen foundation, the Wihuri fund of the Research Foundation of TKK, the Finnish Society of Automation, the Walter Ahlström foundation and TKK. All this support[1] is very gratefully acknowledged.

If one were to write a thesis single-handedly, it surely wouldn't go as swiftly as it did in my case. I therefore wish to acknowledge the distinguished gentlemen **Olli Haavisto** and **Lasse Eriksson** for their good advice on several practical issues and especially for setting an example. I am also very thankful to **Veikko Sariola** for proofreading the thesis manuscript.

Finally, I want to thank those close to me who made me go for it, until the end. You know who you are. Thanks.

Antti Pohjoranta

[1]By the end of February 2010, I had received approximately a gross 145600 euros as salaries and grants. Note, though, that the funding provided by TEKES and GETA is significantly larger due to the included auxiliary expenses also covered by the funding.

List of Publications

[P1] Pohjoranta A., Tenno R., A Method for Microvia-Fill Process Modeling in a Cu Plating System with Additives, *Journal of the Electrochemical Society*, Vol. 154, N:o 10, pp. D502–D509, 2007

[P2] Tenno R., Pohjoranta A., An ALE Model for Prediction and Control of the Microvia Fill Process with Two Additives, *Journal of the Electrochemical Society*, Vol. 155 N:o 5, pp. D383–D388, 2008

[P3] Pohjoranta A., Tenno R., A Computational Multi-Reaction Model of a Cu Electrolysis Cell, *Electrochimica Acta*, Vol. 54, Iss. 24, pp. 5949–5958, 2009

[P4] Pohjoranta A., Mendelson A., Tenno R., A Copper Electrolysis Cell Model Including Effects of the Ohmic Potential Loss in the Cell, *Electrochimica Acta*, Vol. 55, Iss. 3, pp. 1001–1012, 2010

[P5] Tenno R., Pohjoranta A., Microvia Fill Process Control, *International Journal of Control*, Vol. 82, N:o. 5, pp. 883–893, 2009

[P6] Tenno R., Pohjoranta A., Exact Controls for Superconformal Via Fill Process, In proceedings of the *UKACC International Conference on Control 2008*, p. 6, Oxford, UK, 2008

[P7] Pohjoranta A., Tenno R., Implementing surfactant mass balance in 2D FEM-ALE Models, *Engineering with Computers*, p. 12, accepted for publication February 13 2010

[P8] Pohjoranta A., Tenno R., Modelling of Surfactant Mass Balance for Microvia Fill Monitoring, In proceedings of the *International Symposium on High Density Packaging and microsystem integration (HDP'07)*, pp. 198–201, Shanghai, China, June 26.-28., 2007

[P9] Tenno R., Pohjoranta A., Microvia Fill Ratio Control, In proceedings of the *IEEE International Symposium on Industrial Electronics*, pp. 153–156, Vigo, Spain, June 4.-7., 2007

Symbols and abbreviations

Symbols

A_e	Area of electrode e (m^2)
a_i	Activity of species i (dimensionless)
α_i	Apparent transfer coefficient of process i (dimensionless)
b	Constant coefficient (1/s)
c_i	Concentration of species i (mol/m^3)
c^0_{Cu}	Referential concentration of the Cu^{2+} ion, 1000 mol/m^3
c^{lim}	A limit concentration of the Cu^{2+} ion, 3.5 mol/m^3
D_i	Diffusion coefficient of species i (m^2/s)
D_s	Surface diffusion coefficient (m^2/s)
dA, ds	Infinitesimal area element (m^2) or line element (m), respectively
E_{OUT}	Output voltage of an electrolysis cell power source (V)
η_e	Overpotential on electrode e (V)
F	Faraday's constant, 96485 As/mol
$\mathbf{F}$	The deformation gradient (matrix, dimensionless)
f	A generic scalar variable
ϕ	Electric potential (V)
ϕ_{SHE}	The standard hydrogen electrode reference potential, 0 V
$\Delta\phi_e$	Electrode potential vs. the standard hydrogen electrode (V)
$\Delta\phi_{eq,e}$	Equilibrium potential of the copper redox reaction at electrode e (V)
$\Delta\phi^{\ominus}_{eq}$	The standard potential of a redox reaction (V)
$\mathbf{G}$	A generic vector-valued variable
Γ	Surface concentration (mol/m^2)
h_B, h_V	Thickness of copper deposit on the level Board surface and at the micro$V$ia bottom (m)
H	Microvia hole depth (m)
I_{CELL}	Electrolysis cell current (A)
i_e	Current density on electrode e (A/m^2)
$i_{0,e}$	Exchange current density of the reaction on electrode e (A/m^2)
$\mathbf{I}$	Identity tensor
J^u_i	Cost function for control or optimization
k	Shorthand for $z_{\mathrm{Cu}}F/R/T$. At 25°C, k=77.85 1/V.
k^j_i,	Rate coefficient associated to a surface mass transfer process j of species i ($m^3/mol/s$, 1/s, mol/m^2)
k_1, k_2	Weight parameters in cost function
M_i	Molecular mass of species i (kg/mol)
N^j_i, N^j	The mass flux associated to a surface mass transfer process j of species i ($mol/m^2/s$)
n_i	Rate of a reaction i at an electrode surface and the mass flux of the species associated with this reaction ($mol/m^2/s$)
$\mathbf{n}$	Model boundary outward normal vector (dimensionless)

Ω	Model domain
$\partial\Omega$	Model domain boundary
R	Ideal gas coefficient, 8.314 J/mol/K
R_i	The mass flux of species i associated to a chemical reaction (mol/m^3/s)
r, r_{end}	Fill ratio and end-time fill ratio of microvia fill process (no dimension)
ρ_i	Density of species i (kg/m^3)
σ	Conductivity of the electrolyte (S/m)
T	Temperature (K)
t	Time (s)
U_Ω	Voltage drop related to the ohmic resistance of the electrolyte (V)
$\mathbf{v}$	Mesh movement velocity (vector, m/s)
$\mathbf{X}$	The location in the referential two-dimensional, Cartesian coordinate system with the individual coordinates X and Y (m)
$\mathbf{x}$	The location in the current two-dimensional, Cartesian coordinate system with the individual coordinates x and y (m)
z_i	Electron number of species i (dimensionless)
∇_T	Surface tangential differential operator ($\nabla_T = (\mathbf{I} - \mathbf{nn}^\mathsf{T}) \cdot \nabla$)
:	A scalar product operator

Selected subscripts

T	Refers to a surface term (T as in *tangential*)
Cu	Cu^{2+} ion or metallic copper
SHE	Refers to the standard hydrogen electrode potential

Abbreviations

ALE	Arbitrary Lagrange-Eulerian
CEAC	Curvature enhanced accelerator coverage
CAD	Computer aided design
DC	Direct current
FEM	Finite element method
FR	Fill ratio (of a via)
MLB	Multilayered printed circuit board
ODE	Ordinary differential equation
PCB	Printed circuit board
PDE	Partial differential equation
Redox	Reduction-oxidation
SEM	Scanning electron microscope
SHE	Standard hydrogen electrode
TKK	Helsinki University of Technology, the institute known since the beginning of year 2010 as Aalto University School of Science and Technology

Contents

Abstract **iii**

Tiivistelmä **v**

Preface **vii**

List of Publications **viii**

Symbols and abbreviations **xi**

Contents **xiii**

1 Introduction **1**
1.1 Background and motivation 1
1.2 Methods and tools 3
1.3 Thesis contributions 5
1.3.1 Contributions of the Author 7

2 Copper electroplating and microvia filling **9**
2.1 Electroplating concepts 9
2.2 Modeling the electroplating system 13
2.2.1 The electrode-electrolyte interface 13
2.2.2 Coupling the electrode interfaces 14
2.2.3 The electrode models 15
2.2.4 Mass transfer in the electrolyte 21
2.2.5 The mass transfer boundary conditions 23
2.2.6 The mass transfer models 24

3 The microvia fill process **26**
3.1 Overview 26
3.2 Microvia fill chemistry 30
3.2.1 The main additive components 31
3.3 Surface mass balance of the additives 34
3.3.1 Adsorption and desorption of surfactants 37
3.3.2 Consumption of surfactants 39
3.4 Computational modeling of microvia filling 39
3.4.1 The ALE method as applied in this thesis 41
3.4.2 Weak formulations 44
3.4.3 Microvia fill model output 46
3.5 Microvia fill process control simulation 46

4 Summary of the thesis **50**
4.1 The main results 51

5 Conclusions **53**

References **55**

Appendix: Publications **63**

1 Introduction

This thesis presents means for computational modeling of the microvia fill electroplating process system in the context of practical printed circuit board production.

1.1 Background and motivation

A printed circuit board (PCB) is rarely visible to the electronics end-user. Still, a PCB is the backbone of practically every electronics appliance there is. The main purpose of the PCB is to simultaneously function as the chassis for mounting the electronic components of a device, as well as the circuitry between the components. Day-by-day, the gadgets become smaller, lighter and more versatile, and an increasing amount of digital components are crammed into those ever shrinking packages. The PCB that is carrying the components should be able to bear the load both mechanically and in the sense of signal bandwidth.

The continuous progress in complexity and interconnect density of PCB structures has been the driving force and motivation behind all the research discussed in this thesis. The research originated in the computational modeling of the microvia fill process – the manufacturing process where the metallic interconnections between adjacent signal layers of a multilayered PCB are made. This is a complex copper electroplating process, whose outcome depends on numerous factors, including the process conditions and the characteristics of the product itself. Indeed, the original and rather ambitious objective of this thesis was an *automated model-based control system that can guarantee the output quality of the microvia fill process even as the production circumstances and the product design change.*

Developing the process model of microvia filling in a single isolated microvia requires thorough understanding of the computational system that is utilized to model the microvia shape change during electrodeposition. Therefore, a part of the thesis work focused on this topic. Similarly, in order to bring the microvia fill process model into the context of practical PCB manufacturing, several problems related to modeling copper electroplating systems in general needed to be worked out. Lastly, in order to utilize the developed process models for model-based control, appropriate control strategies needed to be developed and tested. The thesis work covers the parts that are necessary to construct a complete system level model of the microvia fill electroplating process and its control.

The motives for developing new microvia fill process models and a model-based

control system for the process are mainly financial and technological. Though some environmental benefits are gained through the increase in output quality and process reliability, the single most important reason for a PCB manufacturer to improve its production line is to remain competitive in the business. On one hand, a better understanding of the microvia fill process enables squeezing more performance out of the manufacturing line and thus improves production efficiency. On the other hand, improving the process itself and being able to better control it brings a technological advantage, in other words, enables manufacturing smaller and more complex products. Since microvia filling is a core process in PCB manufacturing, which is a major segment in the vast industry of electronics manufacturing, it is clear that even minor improvements in the production process can manifest as significant gains in the financial performance of the company. Furthermore, the individual processes on a PCB manufacturing line are still monitored and controlled predominantly by human process operators, whereby the improvement potential of an automatic process control system still remains unexplored. By providing components that are essential to such a process control system, this thesis work aims to help utilizing that potential.

Technological prospects

At the time of writing, a multilayered circuit board may contain more than 50 layers of wiring and the thickest boards are ca. 1 cm in thickness. For the apparent reason, these are mainly used in stationary applications like telecommunication base stations. Boards in mobile appliances can have up to 32 layers, still totaling only 4 mm in thickness. In these boards, the interconnections formed of stacked-up microvias can pass through the whole board. The microvia hole diameter is decreasing towards 50 µm and beyond, with the hole aspect ratio being around one. The number of embedded active and passive components will only increase. It is clear that manufacturing such boards is a challenging task, no matter whether you think of it from the aspect of mechanical or chemical processing. [1]

In current PCB manufacturing lines, copper plating is done in various stages of the manufacturing process. For example, pattern plating, through-hole plating and microvia filling are all done separately, each at a distinct, electrochemical subprocess consisting of several phases. In the future, the huge number of individual steps in the PCB manufacturing process train are reduced in order to cut lead time and costs. One such action is to combine several copper plating processes that are carried out on the same open surface of a PCB-billet, into a single process step. Then, as two or more process steps are integrated into one, there is no doubt that compromises between production criteria have to be made. In practice, designing such production processes purely experimentally and without sophisticated computational tools is ultimately difficult, if not impossible. The need (for a capability) to model, optimize

and control the process will only grow.

1.2 Methods and tools

The emphasis in this thesis is on the practical computational implementation of theories and principles developed by a number of scientists since the 19th century. The main results of the thesis work are computational models that have been validated against experimental data. The backbone of all work is always the empirical data that is collected to keep the model physically plausible.

The approach to modeling the considered processes is mostly based on first principles. Only the estimates for Cu^{2+} ion activity and for the diffusivity of some species are data-based correlation models or semi-empirical estimate equations. When possible, the model parameters have been measured, directly or indirectly, but in many cases the parameters were sought for by fitting the model output with the measured data.

Much of the literature used in this thesis discusses interconnect metallization in the production of integrated circuits (ICs), rather than microvia filling as it is applied in PCB manufacturing. This is because the clear majority of the (published) research work done on the feature filling electroplating chemistry is conducted within, and for, the microchip industry. There, similar electroplating processes as the microvia filling process are utilized to produce copper interconnects for ICs, in the process known as *damascene electroplating*. The main differences between the microvia fill process and the fill processes in damascene electroplating are the hundred-fold difference in scales of time and length of the systems. However, by recognizing this, it is possible to utilize the parts of submicron-scale research that are common to both systems also in microvia fill research. For comparison, a microvia and a nanovia[1], along with the image scales are shown in figure 1.1.

All models documented in this thesis contain a distributed parameters system part. That is, every model includes a part that is described by partial differential equations (PDEs). The computational implementation of the distributed parameters models created in this work is done by utilizing the two (great) software tools of MATLAB ® and COMSOL Multiphysics ®[2] [4, 5]. MATLAB is a versatile tool for numerical computation, which functions well together with COMSOL. COMSOL, then again, is a commercial PDE system solver, which includes a CAD drawing tool

[1] The terms *microvia* and *nanovia* are used to distinguish between cases where the via dimensions are measured in micrometers or in nanometers. Just *via* is used when the meaning is general or clear upon the context.

[2] COMSOL Multiphysics ® was formerly distributed as FEMLAB ®.

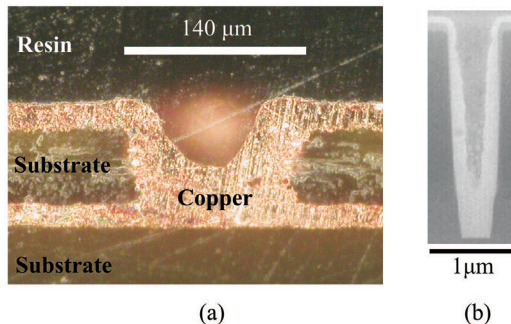

Figure 1.1: Cross-sections of a typical partially filled microvia (a) and nanovia (b). Figure (a) is taken with a digital camera through an optical microscope, whereas figure (b) is a scanning electron microscope photograph [2, 3].

for configuring model geometries. These two programs are generally used in parallel to (i) draw the PDE model geometries, to configure the model physics and to solve the resulting PDE systems (COMSOL), as well as to, (ii) configure and solve various lumped parameter systems and utility functions applied in the PDE-based models (MATLAB).

The PDE solver in COMSOL is based on the finite element method (FEM), which makes FEM an essential part of the models in this thesis. Another computational method that has an essential role in this thesis work is the Arbitrary Lagrange-Eulerian (ALE) method, which is a mathematical method for including physical shape change processes into computational models. In the thesis models, the ALE method is applied to model the geometry change that corresponds to the electrodeposit growth during the microvia fill process. The ALE method is further detailed in Section 3.4.

A variety of commercial measurement and electroplating equipment was used in early via filling experiments, described thoroughly in [6] and [P1, P2]. The experiments took place during 2005-2006 in the former Aspocomp PCB plant in Salo, Finland. Additionally, cyclic voltammetry and potentiostatic measurements were utilized throughout all of the work during 2005-2009. These experiments were mostly carried out with an in-house electroplating apparatus, constructed in the Control Engineering Group laboratory facilities. A PC-connected data acquisition card, configured with MATLAB, was utilized to control and log the voltage signals. Several experiments to verify the consistency of the in-house system were done in the TKK Department of Chemistry, Laboratory of Physical Chemistry, with up-to-date commercial electrochemical experiment equipment. The approach to build and program the experiment equipment in-house was taken to reduce costs and to save time.

1.3 Thesis contributions

The main contributions of this thesis can be divided into four main categories: (i) the microvia fill process models, (ii) the copper electrolysis system models, (iii) the clarification of how the ALE can be applied for surfactant mass balance problems, and (iv) development and simulation of two microvia fill process control strategies. All the thesis contributions are listed in more detail next, and a description of the author's contributions to the publications is given further in Section 1.3.1.

The contributions related to computational modeling of the microvia fill process are documented in [P1, P2, P8] and include:

- The development and implementation of two different computational models of the microvia fill process, as well as their calibration against empirical data.
- The model-based analysis of the effect of selected parameters related to the surfactant additives in the microvia fill system.
- Several via filling experiments, as well as voltammetric experiments utilized in the model development work.

The contributions of this thesis related to modeling the copper electrolysis cell system are documented in [P3, P4, P1] and include:

- A validated model that describes the overall copper reduction-oxidation (redox) reaction with a two-step reaction mechanism in a system with multiple chemical reactions taking place concurrently. The model enables examining the rates of both of the copper redox step-reactions in the none-equilibrium copper redox system, therefore, providing a tool for detailed mechanism study.
- A validated copper electrolysis cell model, whose structure enables including the ohmic loss of potential over the electrolyte into the model, and accounting for its effects on the copper redox systems on both electrodes of the electrolysis cell.
- An estimate for the Cu^{2+} ion activity, which was created based on literature data and verified with potentiostatic measurements.
- The demonstration and examination of using a three-dimensional (3D) electric field model to estimate the ohmic loss in an in-house crafted electrolysis cell, and to create a lumped model of the cell ohmic loss.

- Several voltammetric experiments on copper electrodes used to calibrate and to validate the cell system models.

Contributions related to the application of the Arbitrary Lagrange-Eulerian method for solving surfactant mass balance problems on a deforming surface are documented in [P7, P1, P2, P8]. These contributions include:

- Formulating the problem and implementing the microvia fill process models so that the ALE method is applied and integrated into the system model.
- The analysis and clarification of how the mass balance of a surfactant attached to a deforming surface should be computed in models that are created based on the ALE-FEM framework.
- The examination and explicit formulation of the boundary differential variables and the local surface area as well as its relation to the surface curvature and the surface movement velocity in two-dimensional ALE-FEM models.

The contributions related to the simulation-based design of microvia fill process control are documented in [P5, P6, P9] and include:

- The utilization of distributed parameters models for the design of model-based microvia fill process control.
- The development and simulation of a control strategy, where online nonlinear control of the cathodic current density is utilized to regulate the copper deposit growth inside a microvia during the deposition process and, thereby, to accurately control the end-time via fill ratio to a desired value.
- The development and simulation of a control strategy for model-based optimization of two real properties (process duration, output quality) of the industrial microvia fill process, by manipulating two real process control parameters (plating time, cathode current density).

All these contributions together not only increase the knowledge of modeling the electrochemical microvia fill process, but also lower the threshold to actually applying such models in the design and control of real, industrial microvia fill processes. Because all the models have been implemented using software tools that are commercially available to everybody, adopting these models for process development is significantly more straightforward, than if the models were implemented as in-house program code. Furthermore, the structures of the models are generic in the sense

that modifying them for a different type of process chemistry is simple, regardless of what the exact chemicals included in the chemistry are, as long as their characteristic functions are similar to those included in the models.

1.3.1 Contributions of the Author

The author had an active role in all parts of the work reported in this thesis, except for in completing the computation sequences required for the control system simulations reported in [P5, P6]. These computations were carried out by Robert Tenno. The writing work of the article texts for [P1-P4, P7, P8] was done by the author, under the supervision of Prof. Tenno, whereas the texts for [P5, P6] were written together by both the author and Tenno, and [P9] is mostly written by Tenno. The author's contributions related to the content of the publications are further detailed below.

Publications [P1], [P2] and [P8] introduce two models for simulating the microvia fill process in an isolated, ca. 100 µm-wide microvia. The computational techniques used to implement the microvia fill process model, and the weak-form formulations of the relevant model equations are described. Several chemical experiments that are utilized to create estimates for the activity, diffusivity and adsorption and desorption of the included species are also documented in the articles. Also a simplified surface area -based method to replace curvature computation is given.

The author implemented the computational models, as well as formulated and implemented the area element computation mechanism. The author also formulated the weak-form equations for the surfactant mass balance computation, as well as developed the computer scripts necessary for the simulation sequences utilized in the parameter sensitivity analysis of the microvia fill model. All the experimental work presented in the articles, as well as formulating the diffusivity estimates and the Cu^{2+} ion activity estimates given in the article, was carried out by the author.

Publications [P3] and [P4] discuss the computational modeling of copper electrolysis. A model of the copper electrodeposition process in an aqueous medium, with the copper redox reaction modeled with a two-step mechanism and with multiple concurrent chemical reactions included, is given in [P3]. A copper electrolysis cell model that enables estimating the electric potentials of both electrodes based on only the cell power source output, simultaneously accounting for the effects of electric potential loss in the bulk electrolyte, is given in [P4]. Both models presented in the articles are calibrated and validated against experimental data. A three-dimensional electric field model of the experiment cell is also presented in [P4], and this model is utilized to create an estimator function for the electric potential loss

in the cell bulk electrolyte.

The author created, formulated and implemented the models, as well as carried out all experimental work related to these publications. However, the initial idea for utilizing the Lambert W -function in [P4], as well as some related initial formulations for the current density equations came from Alexander Mendelson.

Publication [P7] documents the main points of a thorough examination to how the computation of surfactant mass balance in a model based on the finite element method (FEM) and the Arbitrary Lagrange-Eulerian (ALE) method can be implemented. The computational techniques behind the surfactant mass balance computation are examined and clarified by simulations. As a result, a formulation that is computationally more stable around boundary singularity points than the original formulation is given for the governing equation of the surfactant surface concentration.

The author carried out all work related to the publication. It should be noted, however, that through the years, significant support related to the practical application of the ALE method was given by the people at COMSOL Oy, Helsinki, Finland.

Publications [P5], [P6] and [P9] present a thorough simulation-based study of utilizing model-based control to manage and to optimize a practical microvia filling process. Two different control strategies are described in the articles. One strategy is designed for always obtaining a desired via fill ratio and the strategy is based on regulating the copper deposit growth velocity by manipulating the cell voltage, so that the behavior of the fill ratio becomes predictable in time. The other strategy enables optimizing the process duration and output quality by manipulating two practical process control parameters, namely the cathode current density and plating time. Both control systems are nonlinear. The control systems are simulated in various cases and the strategies are shown adequate, in the limits of model accuracy.

The models utilized for the control simulations are those mainly developed by the author. The author also developed the scripts that are applied for the consecutive solving of the model PDE system during the parameter search, and completed the work in [P5] with parts related to the chemistry and to the Arbitrary Lagrange-Eulerian method. Mostly the work for these publications was carried out in co-operation of the author and Robert Tenno.

2 Copper electroplating and microvia filling

This section goes through the basic theory related to copper electroplating of PCBs as it is considered in this thesis. The basic terminology and concepts are introduced first in Section 2.1 and the analytical treatment of these concepts is then discussed in Section 2.2. Subsections 2.2.3–2.2.6 will go through how the general theory of electroplating is applied in the models of this thesis, including the utilized simplifications and approximations. Some corners are cut in the presentation of the subjects but this approach is chosen deliberately as the aim throughout the whole work is to create functional computational models of electrochemical systems instead of, e.g., developing elaborate theories of electrochemical kinetics. Consequently, the main contributions of this thesis to the subject of electrochemistry are in the field of computational modeling of electrolysis systems documented in [P3, P4].

2.1 Electroplating concepts

Copper electroplating is the deposition of dissolved copper ions on a PCB by using an electric field[3]. Even the strictest description would touch a wide range of fields in science and technology, and this section gives only a brief look into the basic concepts relevant to copper electroplating as it is applied in the microvia filling process. For the interested reader, there is abundant literature available on both electroplating [e.g., 8, 9] and PCB manufacturing [e.g., 10, 11], as well as the basic electrochemical theory and its practice [e.g., 12–14].

Manufacturing of modern multilayered PCBs is a complex mixture of mechanical, optical, chemical and electrochemical processes. Though everything happens according to a rigorously designed and controlled sequence, even an industry handbook states that attempting to visualize this process can be overwhelming [11, p. 27.37]. Within the PCB manufacturing process sequence, the microvia fill process is *the* copper electroplating process, where the microscopic holes in the boards are filled with copper to create the interconnects between the adjacent board layers.

The microvia fill process equipment - like all electroplating process equipment - consists of an apparatus that includes (i) the electrodes, (ii) the electrolyte and (iii) the electric power source, all constructed inside and around a container tank. The electrodes are immersed in the electrolyte, the power source is connected to the electrodes and the whole set-up is referred to as the electrolysis cell. The text-book illustration of a typical electrochemical cell system is shown in figure 2.1 and a real

[3] Loosely adopted from the definition of *electrodeposition* given by IUPAC in [7]

(laboratory-scale) electrolysis apparatus is shown in figure 2.2. As the power is

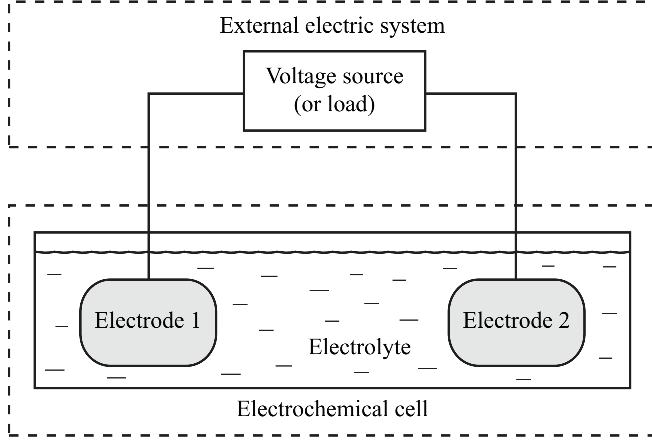

Figure 2.1: A schematic text-book illustration of the electrolysis cell system and its components. Whether electrode 1 is the anode and electrode 2 the cathode, or vice versa, is determined by what poles of the voltage source the electrodes are connected to.

switched on, a difference in the electric potential forms between the electrodes and a current begins to flow from the electrode in a higher potential, the anode, to the electrode in a lower potential, the cathode.

In the microvia fill process, the PCB being plated forms the cathode and, therefore, there is a copper metal cathode in the system. In PCB manufacturing it is still common that also the anode is made of copper, but also an insoluble anode made of, e.g., platinized titanium or iridium oxide coated titanium may be used [11, 15, 16]. In this thesis only a soluble copper metal anode is considered, because this was the case in practice too when the research initiated.

The electric potential difference between the electrodes enables for the copper ions in the electrolyte and the copper atoms in the electrodes to transfer phase and state of charge, according to the copper redox reaction (2.1). By making the PCB the cathode and having copper ions available in the electrolyte, metallic copper is deposited on the PCB according to (2.1) towards the right.

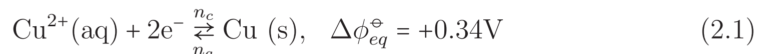

$$\mathrm{Cu}^{2+}(\mathrm{aq}) + 2\mathrm{e}^- \underset{n_a}{\overset{n_c}{\rightleftarrows}} \mathrm{Cu\ (s)}, \quad \Delta\phi_{eq}^{\ominus} = +0.34\mathrm{V} \tag{2.1}$$

In (2.1), the n_a and n_c are the rates of the copper redox reaction (mol/s/m^2) towards the anodic (oxidizing) and cathodic (reducing) direction, respectively, at the considered electrode surface. $\Delta\phi_{eq}^{\ominus}$ is the reaction standard potential, discussed in Section 2.2.1, equation (2.4).

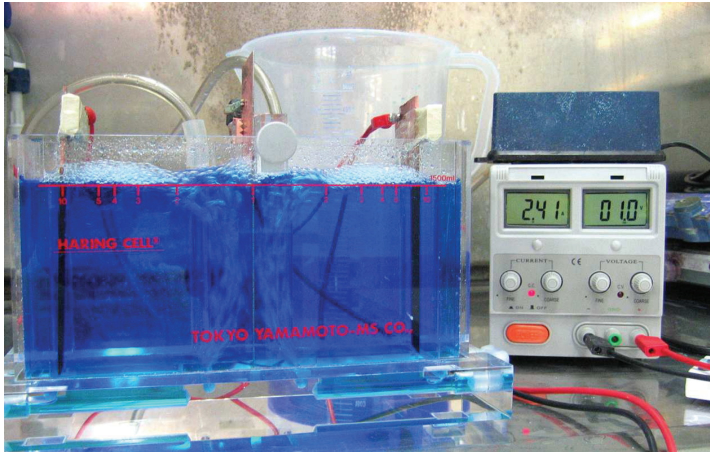

Figure 2.2: A small-scale copper electrolysis system used in, e.g., laboratory-scale via filling experiments. The electrolyte shown in the picture is an acidic copper sulfate electrolyte, thus the blue color. There are three electrodes. The two anodes are in the ends of the cell and they are connected to the same pole in the power source output. The cathode is in the middle and the electrolyte at the cathode is mixed with air bubble agitation. The construction is identical to an industrial PCB plating system, only significantly smaller. The DC power source is in the background, showing a cell voltage of 1.0 V and a current of 2.41 A.

The electrolyte solution, which the electrodes are immersed in, is typically an aqueous mixture of mostly copper sulfate ($CuSO_4$) and sulfuric acid (H_2SO_4). Copper sulfate is added to the bath to bring Cu^{2+} ions to the system, and sulfuric acid is included to improve the electric conductivity of the electrolyte. In addition to the main components, several other chemicals, like chlorine and organic additives, are added to the electrolyte to improve the process characteristics (as discussed in Section 3.2). Typically the electrolyte is agitated vigorously in order to improve mass transfer of the reactive species to and away from the electrodes. As a result of the agitation, the electrolyte composition is very even everywhere in the system, except for very close to the electrode surfaces.

As will be shown further in the text, the rate n_c depends on several variables like the Cu^{2+} ion concentration on the electrodes, the electric potential difference between the electrodes and on what chemicals are put into the electrolyte. Furthermore, it is reasonable to say that the main challenge in administrating the microvia fill process is exactly that of controlling the rate n_c at various locations on the PCB and under various process conditions.

As copper ions are reduced into metal atoms on the cathode, and vice versa on the anode, both mass and charge are transferred over the metal-electrolyte interface and work is done in the process. Similarly, as the ions in the electrolyte carry

current from one electrode to another, more work is done. Energy for this work is brought to the system as the electric potential difference, imposed between the electrodes by the electrolysis power source. The geometric and physico-chemical properties of the system determine how the total potential energy provided to the system by the power source is actually divided into different potential components, corresponding to the work done at the various subprocesses in the system. By distinguishing these subprocesses, it is possible to consider them individually (at first), which simplifies the treatment of the system significantly. In this work, three subprocesses are classified and positioned in the system as follows:

1. The transfer of charge and mass over the cathode-electrolyte interface

2. The transfer of charge and mass over the anode-electrolyte interface

3. The carrying of current through the bulk electrolyte solution

Figure 2.3 illustrates the electric potential steps listed above. In figure 2.3, E_{OUT} is the power source output voltage (V) and I_{CELL} is the cell total current (A). The η_a and η_c are surface overpotential terms, which describe the potential difference over the electrode-electrolyte interface required to obtain the cell current I_{CELL} and similarly, U_Ω describes the potential difference required to carry this current through the non-ideally conducting electrolyte. In practice, the cell must constantly be at a dynamic equilibrium, so that the total electric current at every point of the cell circuit is equal (Kirchoff's current law), and the sum of all potential components over the circuit equals zero at all times (Kirchoff's voltage law). Figure 2.3 illustrates these variables in the system and the equations to calculate the numerical value of these variables are discussed further in the text.

Naturally, the above-presented classification of the subprocesses included in an electrolysis system is only a simplification. For instance, the effects of the so-called electrochemical double-layer and the resulting (non-Faradaic) currents are not considered at all. Consequently, the thesis models are not as such applicable to, e.g., pulse-plating processes, though they technically are solvable even under pulse plating conditions.

All the *potentials* mentioned in the discussion more accurately refer to potential differences vs. a reference point. According to the common convention, also in this thesis the physical system known as the standard hydrogen electrode (SHE) is chosen as the reference point, and is said to have a standard potential of 0 (V) [7].

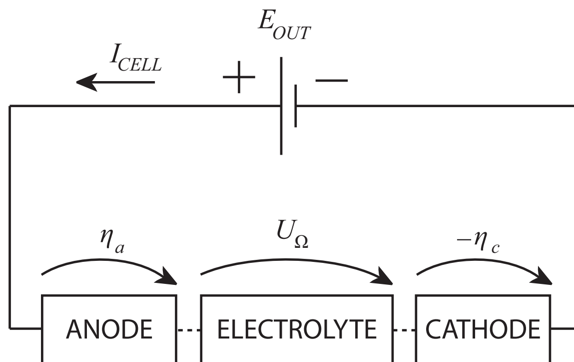

Figure 2.3: A simplified schematic illustration of the potential components in an electroplating cell. The "ANODE" and "CATHODE" boxes refer to the metal-electrolyte interfaces at the electrodes. The sign of the potential difference over the cathode-electrolyte interface is changed, in order for the potential step arrow direction to match the current direction.

2.2 Modeling the electroplating system

2.2.1 The electrode-electrolyte interface

Since the reaction in (2.1) is an electrochemical reaction, in which also charge is transferred, a Faradaic current density i_e (A/m^2) is associated to the reaction rate n_a at the electrode e. Specifically, $i_e = n_a F z_{\mathrm{Cu}}$, where F is the Faraday constant (96485 As/mol) and z_{Cu} the number of electrons transferred in each reaction.

The rate, at which the copper redox reaction (2.1) takes place at an electrode interface, depends on the electric potential difference over the interface. Or more precisely, the rate n_a depends on how much the potential difference over the electrode-electrolyte interface deviates from its equilibrium value, and this potential deviation is referred to as the electrode overpotential, denoted by η_e on the electrode e. Given that the current density i_e is related with a certain reaction rate n_a, which again depends on the potential difference η_e, it follows that i_e can be expressed as a function of η_e with an equation known as the Butler-Volmer equation, (2.2).

$$i_e = i_{0,e}\left(a_{a,e}e^{k\alpha_{a,e}\eta_e} - a_{c,e}e^{-k\alpha_{c,e}\eta_e}\right) \tag{2.2}$$

In (2.2), $i_{0,e}$ is the exchange current density (A/m^2) of the reaction at electrode e, and the activity of the reactants involved in the reaction towards either the anodic or the cathodic direction is denoted by $a_{a,e}$ and $a_{c,e}$, respectively, (dimensionless). The coefficient k is a shorthand for $z_{\mathrm{Cu}}F/R/T$, (1/V), where R is the ideal gas constant (8.3145 J/mol/K) and T the temperature (K). The two parameters $\alpha_{e,a}$ and $\alpha_{e,c}$ in (2.2), are the apparent transfer coefficient of the charge transfer reaction on electrode

e, for the anodic (a) and cathodic (c) reactions, respectively (dimensionless). These describe the (a)symmetry of the copper redox reaction, i.e., whether the reaction towards the cathodic or towards the anodic direction is more sensitive to changes in the electrode potential.

As mentioned, the potential difference η_e (V) in (2.2), also depicted in figure 2.3, describes how much the potential difference over the metal-electrolyte interface ($\Delta\phi_e$) deviates from its value when the interface is in thermodynamic equilibrium ($\Delta\phi_{eq,e}$). η_e is calculated with (2.3)

$$\eta_e = \Delta\phi_e - \Delta\phi_{eq,e}, \tag{2.3}$$

where ϕ is the electric potential (V). The potential differences $\Delta\phi_{eq,e}$ and $\Delta\phi_e$ are considered with respect to the SHE, i.e., $\Delta\phi_{eq,e} = \phi_{eq,e} - \phi_{SHE}$ and $\Delta\phi_e = \phi_e - \phi_{SHE}$. This enables coupling the electrochemical potential steps with the electric potentials steps observed in the system. The $\Delta\phi_{eq,e}$ term is the equilibrium potential (V) of the metal-electrolyte interface at electrode e, and it is evaluated upon the Nernst equation (2.4).

$$\Delta\phi_{eq,e} = \Delta\phi_{eq}^{\ominus} + k^{-1}\ln(a_e) \tag{2.4}$$

In (2.4), $\Delta\phi_{eq}^{\ominus}$ is the standard potential of reaction (2.1), (+0.34 V), describing the equilibrium potential of the copper metal-electrolyte interface in standard conditions, vs. the SHE. With these definitions, the whole potential system is well defined with respect to a single reference point, given by a well defined electrochemical system, the SHE.

2.2.2 Coupling the electrode interfaces

As the circuit shown in figure 2.3 lets assume, the current densities i_e and the potential differences η_e over each electrode-electrolyte interface are connected. Therefore, when considering the whole electrolysis cell with two electrodes, two coupling conditions can be formulated based on the assumption of electrodynamic equilibrium.

Firstly, as only one current runs in the cell circuit (figure 2.3), the total current over both electrode-electrolyte interfaces (directions considered) must be equal on both electrodes at each time instant. Therefore, the current density on the anode multiplied by its area must be equal (but opposite-signed) to that on the cathode. If the electrode surface area (m^2) is denoted by A_e,

$$A_a i_a + A_c i_c = 0. \tag{2.5}$$

Secondly, the sum of all potential steps over the electrolysis circuit must equal zero.

Therefore,

$$E_{OUT} + \eta_a - \eta_c + U_\Omega = 0 \tag{2.6}$$

The sign of η_c is changed here, since the potential difference is always measured with respect to the direction of current. If considering the Butler-Volmer equation (2.2) on both of the electrodes and the cell current simultaneously, the sign of one of the overpotential steps must be changed.

2.2.3 The electrode models

The simplified Butler-Volmer equation models

The bi-directional Butler-Volmer equation (2.2) is the starting point for calculating the current density i_e and estimating the rate n_a on an electrode, at a given potential η_e. The equation is called bi-directional, because it yields the electrode current density correctly, irrespective of the sign of the electrode overpotential η_e. Unfortunately, as such (2.2) is inherently nonlinear and rather unsuitable for further analytical usage. Due to the form of (2.2), however, one part of the right-hand-side will always decay towards zero as the absolute value of η_e grows and, therefore, the equation can be simplified by considering it separately for each sign of electrode overpotential. In practice this means that the approximations

$$i_e \approx i_{0,e} a_{a,e} e^{k\alpha_{a,e}\eta_e}, \qquad \text{when } \eta_e > 0 \text{ and} \tag{2.7a}$$

$$i_e \approx -i_{0,e} a_{c,e} e^{-k\alpha_{c,e}\eta_e}, \qquad \text{when } \eta_e < 0 \tag{2.7b}$$

are used. This approximation has at some stage been applied in most of the models where the Butler-Volmer equation is used [P1, P2, P4].

The simplification (2.7) is rather well acceptable in many physical systems and enables remaining fully analytical in the treatment, while still utilizing the Butler-Volmer equation for constructing an electrolysis model. The downside is that now the models for each electrode must be considered separately for each case of either positive or negative value of electrode overpotential.

Once approximating (2.2) with (2.7) is accepted it is possible to further analyze the relation between the current density i_e on a chosen electrode and the electrode overpotential η_e. The approximation enables, e.g., investigating the electrode overpotential with a respect to a given electrode current density, corresponding to the case of galvanostatic electrodeposition control [P1, P2], or calculating the electrode current density as a function of the cell power source output voltage [P4]. However, since the approximation (2.7) essentially splits the original bi-directional

Butler-Volmer equation (2.2) into two parts, and each part of the approximation is valid only when the electrode overpotential η_e is either positive or negative, also the electrode models based on this approximation are valid only during either positive or negative values of η_e. For computational purposes, however, this is inconvenient since crossing or approaching the zero-line of η_e is required in many cases like during the initialization of the simulation, and when a strong concentration overpotential is present and the cell power source output is small. Two different methods to overcome this inconvenience that is caused by splitting the system into two parts have been applied in [P1, P2] and [P4].

The first method is to neglect the anodic part (when $\eta_e > 0$) and to use only the cathodic part (when $\eta_e < 0$) of the electrode equation. This approach is justified in [P1, P2] by the fact that only copper electrodeposition in the microvia is examined and, therefore, the electrode only operates on the cathodic potential range. However, in order to improve the system operation close to the zero-potential, the electrode process is assumed symmetric so, that the electrode current on an anodic potential is equal (but opposite-signed) to that on the cathodic part. With this assumption, the electrode current density equation may be formulated by using a hyperbolic sine function [P1, eq. (11), P2, eq. (1)], which is smooth and continuous over the zero-potential area. This improves the model computability significantly.

The other method is to re-superimpose the current density equations that are obtained separately for both the positive and negative values of η_e, after they are derived. This approach yields a similar bi-directional form for the electrode current density approximation that the original Butler-Volmer equation has. The electrode current density equation used in [P4, eq. (25)] was obtained in this manner. The procedure is justified by the fact that - similarly to the original Butler-Volmer equation - the part-wise derived equations [P4, eq. (20) and eq. (24)] approach zero on the parts where they are not valid. That is, the approximation for the anodic part decays to zero when the electrode potential becomes cathodic and vice versa for the cathodic part. However, close to the zero-potential, the superimposed approximations yield a smooth and continuous operation, which again improves model computability.

The approximation (2.7) is not utilized in [P3], but instead the Butler-Volmer equation is solved by using a numerical search algorithm, as described next.

The copper redox system model

In the electrode models described above, the electrochemical reaction system at the electrode-electrolyte interface was considered as the one shown in (2.1). The

reaction in (2.1) is, however, a sum of the two step reactions (2.8) that actually form the copper reduction-oxidation process.

$$Cu^{2+}\ (aq) + e^- \underset{n_{a,1}}{\overset{n_{c,1}}{\rightleftharpoons}} Cu^+, \qquad \Delta\phi^{\ominus}_{eq,1} = +0.16V \tag{2.8a}$$

$$Cu^+ + e^- \underset{n_{a,2}}{\overset{n_{c,2}}{\rightleftharpoons}} Cu\ (s)\ , \qquad \Delta\phi^{\ominus}_{eq,2} = +0.52V \tag{2.8b}$$

A copper electrolysis model that includes these elementary step-reactions of the copper redox reaction is developed in [P3]. The model also takes into account two other concurrently occurring chemical processes; the copper disproportionation/comproportionation system

$$2Cu^+ \underset{n_{cp}}{\overset{n_{dp}}{\rightleftharpoons}} Cu^{2+} + Cu\ (s) \tag{2.9}$$

and the copper sulfate dissolution reaction

$$CuSO_4 \underset{n_{ass}}{\overset{n_{diss}}{\rightleftharpoons}} Cu^{2+} + SO_4^{2-}, \tag{2.10}$$

[P3, eq. (2)-(4)].

In [P3], the dependence between electrode current density and electrode overpotential is described by a separate Butler-Volmer equation for each of the step reactions in (2.8) [P3, eq. (6)], which are then superimposed to obtain the eventual net electrode current density [P3, eq. (7)]. The model enables examining the effects that modifying the reaction rates $n_{i,1}$ and $n_{i,2}$ can eventually have on the copper electrode current density and copper deposition. It is exactly these reaction rates that are influenced by the electrolyte additives in the microvia fill bath. The model, therefore, provides a tool for analyzing the mechanisms of the additive effects. As an example, the current densities corresponding to the reaction rates of the individual reactions during a cell potential sweep is shown in figure 2.4. Further, to illustrate the level of model accuracy, the estimated and measured electrode current densities that correspond to the reaction rates shown in figure 2.4 are plotted in figure 2.5.

Due to the structure of the electrode current density model that is formed based on (2.8), it is not possible to utilize the simplification (2.7). More specifically, since the equilibrium potentials of (2.8a) and (2.8b) are different, there is no single zero-level of electrode overpotential. However, because the reaction rates of (2.8a) and (2.8b) are coupled also by the reagent concentrations, it is possible to find the electrode potential $\Delta\phi_e$, that provides the required electrode overpotentials ($\eta_{e,1}$ and $\eta_{e,2}$) for both step reactions in (2.8) under the prevailing mass transfer conditions. In [P3] this electrode potential is found by using the numerical direct search algorithm `fminsearch`, provided by MATLAB and based on the Nelder-Mead simplex method [5]. As the equation whose minimum is sought for is a simple squared sum of scalar

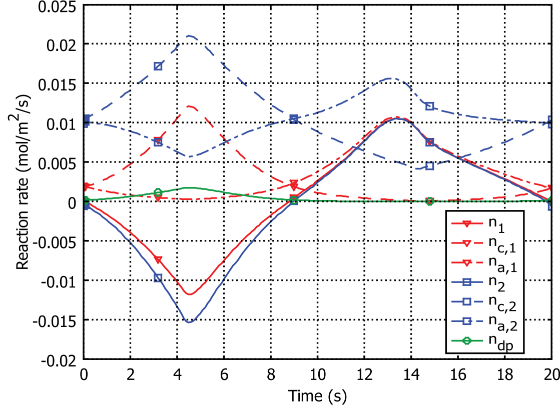

Figure 2.4: The reaction rates of the individual reactions in (2.8) and (2.9) on one electrode surface, during an experiment where the cell voltage changes between ca. +0.5 V and -0.5 V at a rate of 0.1 V/s. (Figure corresponds to [P3, fig. 6].)

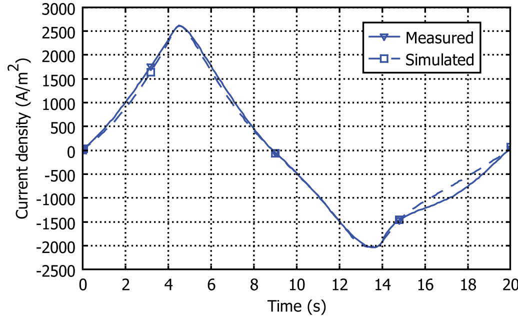

Figure 2.5: The estimated electrode current density and the corresponding measured value on one electrode during the experiment described in figure 2.4. (Figure is extracted from [P3, fig. 13].)

exponential functions, it is low-dimensional and has a global minimum, whereby the search is shown to converge [17].

Including the cell ohmic loss

The ohmic loss of potential over the bulk electrolyte, denoted with U_Ω in (2.6) can not be ignored in a typical copper electroplating bath applied in PCB production. Therefore, a value for U_Ω should be estimated somehow and one method is described in [P4]. In [P4] a scalar estimate for U_Ω is created by utilizing a 3D electric field model of the electrolysis cell [P4, Section 2]. By examining the 3D model, the characteristics of the physical cell structure are then lumped into a scalar estimate

[P4, eq. (5)-(6)]. Reducing the estimate to a scalar function significantly increases the usability of the estimate in further modeling work. In [P4] the estimate is utilized to derive semi-analytical formulations for the electrode current density [P4, eq. (25)] and overpotential [P4, eq. (19) and (23)] as a function of the electrolysis cell power source output voltage. The model, therefore, enables estimating how the cell power source output is divided into the different potential components (shown in figure 2.3) when the system geometry and electrolyte properties are known. As an example, the estimated electrode potentials, as well as the cell ohmic loss estimated by the model in [P4] are shown along the cell voltage in figure 2.6. Based on figure

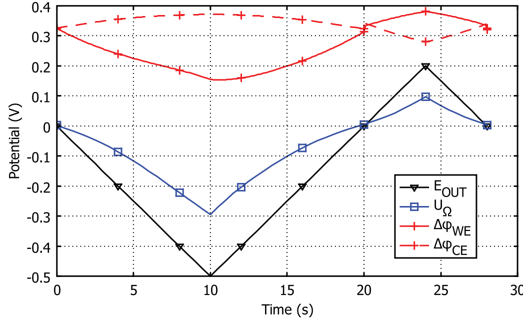

Figure 2.6: The cell power source output voltage (E_{OUT}), the estimated electrode potentials ($\Delta\phi_{WE}$ and $\Delta\phi_{CE}$, vs. SHE) and the estimated cell ohmic loss (U_Ω) during one potential sweep experiment. The cell power source output voltage is the only input variable in the model. [P4]

2.6, it is clear that the cell ohmic loss (U_Ω) is relevant in magnitude compared to the cell power source output (E_{OUT}). To illustrate the effect of the U_Ω term on i_e, the estimated and measured values of the electrode current density on one electrode are plotted in figure 2.7, when three differently-sized cells are used. The cell voltage sweep is the same in all of the experiments.

By examining figure 2.6 closely, a small notch can be observed in the electrode potential curves (red, +) when they pass over the equilibrium potential level. This is because the re-superimposing method, which is utilized to smoothen the electrode current density estimates, cannot be used for the electrode potential estimates. Moreover, if this procedure was used to smoothen the electrode potential estimates, more severe problems than the notch around the equilibrium potential level would occur at other locations due to the characteristics of the Lambert W -function, as explained in [P4, Section 7.1, fig. 11].

The models described in [P1, P2] are not adequate for describing a full microvia electroplating cell since the ohmic resistivity of the electrolyte is essentially ignored in these models. However, the models are adequate for what they are intended to,

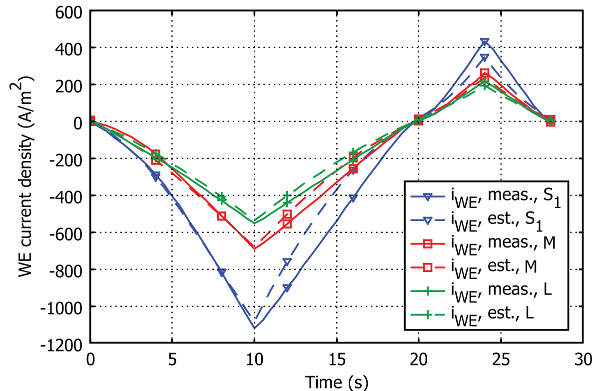

Figure 2.7: The electrode current density (on the working electrode) estimated by the model (dashed lines) and as measured (solid lines) in three different cases of cell dimensions. The cell length changes from 3 cm to 10 cm and to 16 cm between the cases S_1, M and L, while the cell width stays constant and the cell height varies only very little. [P4]

i.e., to examine only an individual, isolated microvia.

Estimating Cu^{2+} ion activity

The activity of Cu^{2+} ions, $a_{c,e}$, appears in several of the above equations. In some systems the activity is approximated directly with the species' concentration, but within this thesis, $a_{c,e}$ is approximated with a data-based equation (2.11) [P1, eq. (5)].

$$a_{c,e} \approx \frac{c_{\mathrm{Cu},e}}{c^0_{\mathrm{Cu}}} \left(\frac{c_{\mathrm{Cu},e} + c^{\mathrm{lim}}}{c^0_{\mathrm{Cu}} + c^{\mathrm{lim}}} \right)^{-0.5554} \tag{2.11}$$

In (2.11), $c_{\mathrm{Cu},e}$ is the Cu^{2+} ion concentration ($\mathrm{mol/m^3}$) at the electrode, c^0_{Cu} is the (chosen) reference concentration of copper, 1000 $\mathrm{mol/m^3}$, and c^{lim} is a limit concentration below which the solution is considered dilute, 3.5 $\mathrm{mol/m^3}$ [P1]. By convention, the activity of the copper metal face is taken as equal to unity ($a_{a,e} = 1$) and, therefore, from here on the symbols $a_{a,e}$ and the letter c for the cathodic reaction are omitted.

The estimate 2.11 gives the nonlinear relationship between the molar concentration and the activity of the Cu^{2+} ion in an aqueous medium. The estimate was developed

based on literature data and verified with measurements. The functioning of the estimate is illustrated in figure 2.8. The figure shows the equilibrium potential of a copper electrode in an aqueous $CuSO_4$ solution measured and estimated in various solution concentrations. Two estimates are plotted; one that accounts for the Cu^{2+} ion activity and one that does not.

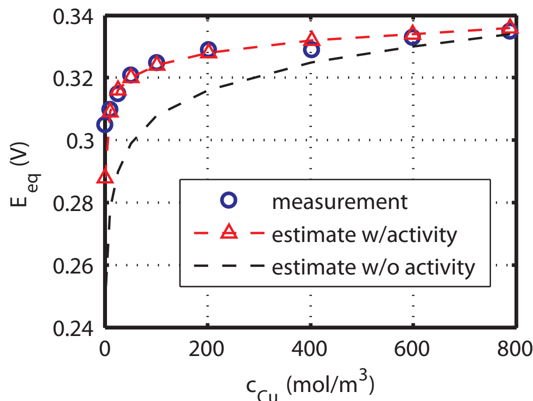

Figure 2.8: The equilibrium potential values of a Cu/Cu^{2+} electrode (in aqueous $CuSO_4$) measured (blue ∘) and estimated with two different estimates. One of the estimates takes into account the effect of the copper ion activity (dashed, red, △) and the other one does not (dashed, black).

The equations from (2.2) to (2.11) effectively compile the theoretical treatment of a single electrode-electrolyte interface, as it is considered in this thesis. When proceeding further from the electrode surface towards the bulk electrolyte, the electric field and mass transfer phenomena included in the system also need to be discussed.

2.2.4 Mass transfer in the electrolyte

By looking at (2.2), (2.4) and (2.11) it is apparent that the Cu^{2+} ion concentration plays a key role in the electrolysis system. The deposition or solution of copper on the electrodes creates a mass flux of copper over the electrode-electrolyte interface, which means that mass transfer of copper ions in the electrolyte phase must be included in the model. Though only the Cu^{2+} ion was mentioned here, the same applies also to other ions as well as to the electrolyte additives that are discussed further in Section 3.2.

In the electrolyte solution, mass transfer of species takes place through convective

mass transport, diffusion and migration, as well as through the chemical reactions of the interacting species. Due to electrolyte agitation, convection is typically dominant everywhere except for very close to the electrode-electrolyte interfaces. In the areas where convection clearly dominates mass transfer, it is often not explicitly modeled but the situation is simplified by assuming that the electrolyte is homogenous there. Explicit modeling of convective mass transfer is also out of the scope of this thesis. Very close to the electrode surfaces, however, the real viscosity of the electrolyte results in a layer of electrode solution where the electrolyte flow velocity is very low ($\approx$ 0 m/s) and mass transfer of species is dominated by diffusion, migration and possibly a chemical reaction taking place between the considered components. This system is known as the Nernst-Planck mass transfer system completed with a reaction term (2.12).

$$\frac{\partial c_i}{\partial t} = \underbrace{\nabla \cdot (D_i \nabla c_i)}_{\text{Diffusion term}} + \underbrace{\nabla \cdot \left(z_i F \frac{D_i}{RT} c_i \nabla \phi \right)}_{\text{Migration term}} + \underbrace{R_i}_{\text{Reaction term}} \tag{2.12}$$

In (2.12), c_i is the concentration (mol/m^3), z_i the electron number (dimensionless) and D_i the diffusivity (m^2/s) of species i. It is clear that if the species is non-ionic, i.e., z_i=0, no migration term is included in its mass transfer computation. This is the case for, e.g., the electrically neutral electrolyte additives. R_i is the rate of creation (or decomposition, mol/m^3/s) of species i, if it takes part in a chemical reaction like (2.10) for example.

The mass transfer of ionic species is further restricted by the strong physical constraint, known as the electroneutrality condition

$$\sum z_i c_i = 0. \tag{2.13}$$

Equation (2.13) states that the electrolyte should at all times stay electrically neutral, when even infinitesimally small volumes are considered. To explain this conversely, it is considered that creating a spatial separation of charge requires a very large amount of energy [12]. When implementing the computational model, (2.13) enables computing the concentration of one species in the system without using a PDE and thereby simplifies the system configuration.

Lastly, since the electric field variable, ϕ (V), is also included in the equation system, it also needs to be solved. Including the electric field into the system is done based on the conservation of charge principle, which states that

$$\nabla \cdot \mathbf{i} = 0, \tag{2.14}$$

where $\mathbf{i}$ is the current density (A/m^2) in the electrolyte. Because the current is carried in the electrolyte only by the ions, $\mathbf{i}$ may be formulated through the mass

flux of the ions as

$$\mathbf{i} = F \sum z_i \left(D_i \nabla c_i + F z_i \frac{D_i}{RT} c_i \nabla \phi + R_i \right). \tag{2.15}$$

Equation (2.15) may be considered significant since it actually is the one that realizes the physical coupling between the electric part and the mass transfer part of the electrolysis cell system, in the electrolyte domain.

2.2.5 The mass transfer boundary conditions

The PDEs (2.12)–(2.15) are the starting point for formulating the mass transfer of the species considered in the electrolysis models in this thesis. However, since the equations are partial differential equations, they require initial and boundary conditions to be determined before a (well-defined) solution can be obtained. The most important boundary condition was, in fact, given already in Section 2.2.1. This is the relation between transferred charge, i.e., current, and reaction rate, i.e. rate of mass transfer, over the electrode-electrolyte interface,

$$i_e = \sum n_{a,i} F z_i. \tag{2.16}$$

Equation (2.16) couples the electric field and the mass transfer system at the electrode interface by giving a physically equivalent Neumann boundary condition for both of these systems.

For the Nernst-Planck mass transfer system (2.12) the boundary condition flux is defined as

$$\mathbf{n} \cdot \left(D_i \nabla c_i + z_i F \frac{D_i}{RT} c_i \nabla \phi + R_i \right) = n_{a,i} \tag{2.17}$$

at the boundary, and the current boundary density condition is defined for the electric field system, so that

$$\mathbf{n} \cdot F \sum z_i \left(D_i \nabla c_i + F z_i \frac{D_i}{RT} c_i \nabla \phi \right) = i_e. \tag{2.18}$$

When possible, simplified boundary conditions may be set, as follows:

- A fixed concentration on a (hypothetical) fluid-fluid interface, where the other fluid is continuously agitated; $c_i = c_0$
- A fixed potential on a boundary that is, e.g., considered to be connected to a power source or to the ground; $\phi = \phi_0$

- An isolation condition or symmetry condition setting the mass flux, given in (2.17), over the boundary to zero ($n_a = 0$)
- An electrical insulation or symmetry condition, setting the current, given in (2.18), over the boundary to zero ($i_e = 0$)

2.2.6 The mass transfer models

In order to implement a physically relevant electrolysis model, the mass transfer system of PDEs and boundary conditions often have to be modified. The application of (2.12)–(2.18) is described next. Simple symmetry conditions or isolation conditions are not detailed below.

In the microvia fill models [P1, P2], only the surface of one electrode is examined and the electrode is assumed to be immersed in a practical microvia fill bath, where the electrolyte is continuously agitated. The boundaries for the model are thus formed by the electrode surface and the solution interface, where convection stops from being the dominant form of mass transfer and (2.12) prevails.

The models in [P1, P2] are further reduced by not considering the electroneutrality condition (2.13). Instead, the mass transfer of each species is solved with (2.12) individually and the electric field is solved separately with the Poisson equation

$$\nabla \cdot (\sigma \nabla \phi) = 0, \tag{2.19}$$

where the conductivity σ (S/m) is computed as

$$\sigma = \frac{F^2}{RT} \sum z_i^2 D_i c_i, \tag{2.20}$$

[P1, eq. (25)-(26)]. Therefore, though the electric field and the mass transfer system are coupled, the equation system (2.12)–(2.15) is relaxed on behalf of the electroneutrality condition. Furthermore, no chemical reactions of species are considered in the electrolyte domain, but only on the electrode surface, and $R_i = 0$ for all species in [P1, P2].

It is known that (2.20) is a sufficient approximation only for the conductivity of very dilute, binary, ionic solutions. This can be considered a shortcoming in the models and a source of model error. However, the benefit of using a concentration-dependent approximation for σ with (2.19), is that with this approximation the electric field *shape* is more accurate than with, e.g., a constant value for σ. For example, by using the concentration-dependent σ-approximation, the resistance of

the electrolyte grows as the electrolyte becomes depleted of ions close to the cathode-electrolyte interface.

The boundary conditions for this system are obtained based on the physical process. Since the process is galvanostatically controlled, a prescribed current density is set on the cathode [P1, eq. (29)] and a constant potential [P1, eq. (28)] is set on the solution interface to account for the electric field boundary conditions. For the mass transfer equations, a mass flux of species is set over the electrode surface [P1, eq. (32)] and a constant concentration of species is set on the solution interface [P1, eq. (31)].

The model obtained with the equation system (2.12), (2.19)–(2.20) together with the boundary conditions is simplified from the original Nernst-Planck model. Nevertheless, it does enable the examination of the mass transfer phenomena, the electric field and the electrodeposit growth inside a single isolated microvia with sufficient accuracy. In [P3, P4] the mass transfer models are created by utilizing the original system description given by (2.12)–(2.15), which includes the electroneutrality condition, and in [P3] also the reaction terms R_i [P3, eq. (11),(12)] are non-zero in the electrolyte domain.

Because the models documented in [P3, P4] are electrolysis cell models, the boundary conditions for the mass transfer and electric field systems are also different from those mentioned in [P1, P2]. In [P3] the potentials of both electrodes are found with a numerical search. Therefore, a fixed potential condition is set on both electrode boundaries [P3, eq. (18)]. In [P4] the boundary condition for one electrode is set as a prescribed current density as shown in (2.18) [P4, eq. (14)], and a fixed potential value is set on the other electrode. The mass transfer boundary conditions in [P3, P4] are set on both electrodes as in (2.17) [P3, eq. (16), P4, eq. (13)].

3 The microvia fill process

This section will first give an overview of the microvia fill process technology and the related electrolyte additive chemistry in Sections 3.1 and 3.2. Then the analytical treatment of the mass balance of species attached on a deforming solid surface, like the copper surface being deposited during microvia filling, is discussed in Section 3.3. An introduction to the practical computational modeling of the microvia fill process is given in Section 3.4. Finally, the microvia fill process discussion is closed in Section 3.5 by a look into the model-based control of the process. The contributions of this thesis to the research of the microvia fill process technology are mostly within the topics discussed in Sections 3.4 and 3.5, that is, in modeling and model-based control of the process, documented in [P1, P2, P5-P9].

3.1 Overview

The microvia fill process is a copper electroplating process and it is only one among the industrially applied technologies for manufacturing the buried interconnections that penetrate individual layers in multilayered PCBs. Various other technologies such as the buried bump interconnection technology (B^2IT) and neo Manhattan Bump interconnection (NMBI) technology exist and are reported in [6, 11]. Overview articles of the microvia fill process as it is applied in practice are given in [18–20].

In microvia filling, the holes required for creating the interstitial interconnections are made on individual board layers by laser ablation (a.k.a. laser drilling). The holes are created so that they reach through the outer copper layer and through one whole layer of dielectric, but do not penetrate the copper layer beneath the dielectric layer. During drilling, the copper layer beneath the dielectric substrate being ablated reflects the beam back so that the holes do not become deeper than necessary. That is, the holes remain *blind*, with the bottom being a clean copper surface and the walls being dielectric. After laser drilling, the walls of the holes need to be made electrically conductive in order to facilitate the actual microvia fill electroplating process. Electroless copper deposition, reinforced with a short, high-current electrolytic copper deposition process, called *flash copper*, is typically used for this. The deposited copper layer are then shortly etched with persulfate or with a sulfuric acid–hydrogen peroxide solution to remove pretreatment contaminants and oxidation, in a process called *microetching* [11]. Finally, before entering the microvia fill electrolysis bath, the copper surface is dipped into sulfuric acid and rinsed, in order to remove microetch residues and to improve the initial surface.

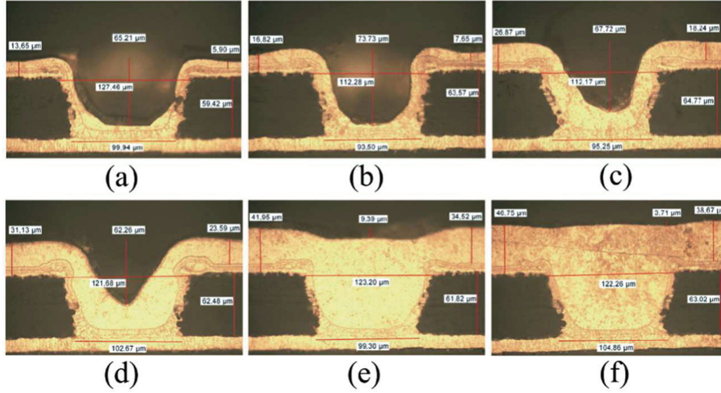

Figure 3.1: Cross-section profile images of microvia samples plated for (a) 15, (b) 30, (c) 45, (d) 60, (e) 75, (f) 90 minutes. The pictures are taken with an optical microscope, with a 500x magnification.

Once the via hole is ready for microvia fill electrolysis, the board is fed into the microvia fill bath. The microvia fill electrolysis might then last from 40 to 70 minutes, depending on the system and the product. An example of how the microvia fill process progresses in time is given in figure 3.1, which shows cross-sections of microvias plated for different amounts of time. A successfully electroplated microvia is filled completely but not excessively, as shown in figures 3.1 (f) and 3.2, thereby leaving a smooth surface for the next circuit layer to be built on.

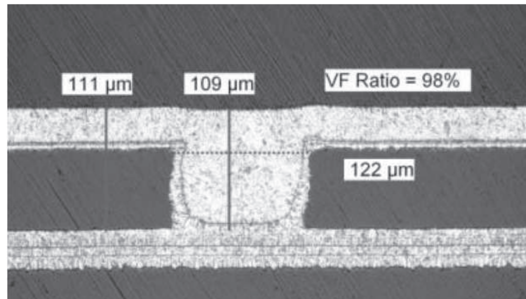

Figure 3.2: A cross-section image of a successfully filled microvia. The picture is taken with a scanning electron microscope. [21]

The microvia interconnects can be hampered by poor contacts to the surrounding layers and an incomplete fill, as shown in figures 3.1 (a)-(e). The smoother the filled via surface is, the better is the contact with the layer built on top. Only partially filled vias and void vias (figure 3.3) eventually create a bottleneck in the current path. This increases the local current density and causes reliability problems due to increased electromigration and resistive heating. Empty vias, caused by gas

entrapment or a poor seed copper layer, interrupt the circuit completely.

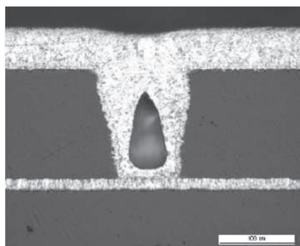

Figure 3.3: A void inside a microvia. [21]

Overfilled and underfilled vias, shown in figures 3.4 and 3.5, respectively, pose a problem in the following steps of the PCB manufacturing process. When the laser ablation of the dielectric layer is done exactly on top of an improperly filled via, the laser beam scatters from the uneven copper surface, and the hole for the next microvia becomes deformed. Unsatisfactory fill of the microvia in the layer stacked on top of the poorly filled via then becomes very probable [21].

Figure 3.4: The cross-section image of two stacked vias, when the bottom via has been overfilled in the previous microvia fill step. The upper layer via has deformed due to the bump on top of the bottom layer via and the created interconnection is unreliable. [21]

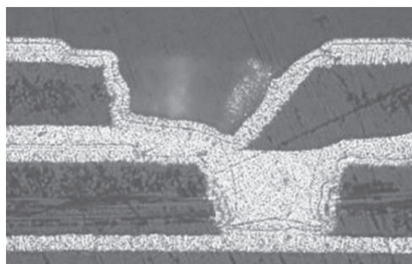

Figure 3.5: An incompletely filled buried microvia has caused the laser beam to deflect asymmetrically from its uneven top surface. As a result, the drilled outer layer hole is malformed. [21]

The level of success, i.e., the quality of the microvia fill process output is difficult to measure in practice. This is due to the vast amount of individual vias on one board and because of the small size of the microvias. Nevertheless, two quantitative measures, called the dimple depth and the via fill ratio, are commonly used. The first one (illustrated in figure 3.6) is a simple measure for fill completeness and

it can be measured without harming the measured object by using, e.g., a laser interferometer. The problem with this measurement method is, however, that no

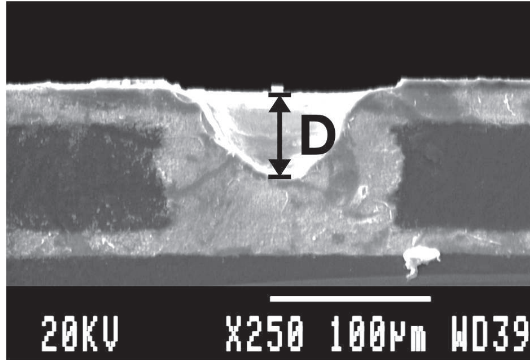

Figure 3.6: D (black arrow) denotes the dimple depth measure of the via.

information of the plated copper layer thickness is obtained. Therefore, when a process output sample can be sacrificed for cross-sectioning, this is done to obtain the via fill ratio of the sample. The via fill ratio (illustrated in figure 3.7) gives information of how the deposit inside the via grows with respect to the copper layer on the board surface. Cross-sectioning the PCB naturally destroys the piece completely and, therefore, this measure cannot be used to monitor the end-product quality. In the publications included in this thesis, the via fill ratio is preferred as the quality measure of the via fill process.

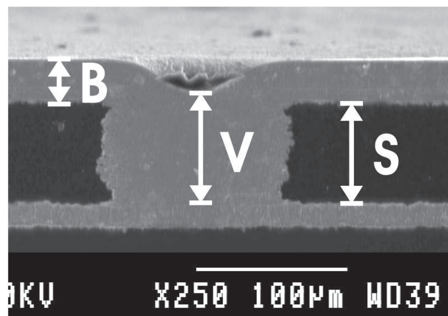

Figure 3.7: B (white arrow) denotes growth of the copper deposit on the PCB surface and V (white arrow) is growth on top of the center of via. S denotes the substrate layer thickness. Via fill ratio, FR, is calculated as $FR = V/(B+S)$.

Several challenges to operating the via fill process are brought by the fact that online monitoring of the process is generally not possible on a detailed level. Major error situations, like equipment breakdown, are detected by the safety systems but

due to the vast amount and the microscopic size of the features on the PCB, the evolution of the microvia fill process cannot be directly measured during the plating process. Therefore, the process operator cannot, e.g., decide on-site to increase the deposition time if unevenly filled vias are observed. Furthermore, since measuring the success of a via fill process after each deposition step would require several thousands of microvias to be examined, a faulty process output cannot be detected before a testing phase, which takes place only after the whole PCB is finished. This means that an error in the microvia fill process might not be discovered before a significant amount of waste is produced.

The properties that the operator of a practical via fill plating system can manipulate to obtain a good fill are practically only two: the average cathode current density and the plating time. Moreover, the average cathode current density is typically obtained by adjusting the plating cell voltage, which means that a change in the desired plating current density essentially affects all the plating system potential components (shown in (2.6)). A computational process model enables pre-examining the effect that manipulating any of these properties has on the process output.

3.2 Microvia fill chemistry

Looking at figure 3.1, the microvia fill process may seem contrary to common sense. Mass transfer of copper ions is surely worse to the bottom of the via than to its mouth or to the level board surface, but still, the deposit growth is fastest inside, and at the bottom of the via. Furthermore, since the electric field tends to intensify at protrusive sites like the via mouth rim, one would expect to see accelerated deposit growth at these sites. Again, however, the opposite is observed in figure 3.1. This unnatural deposit growth, called *superconformal* deposition, is obtained by using electrolyte additives that influence the rate of the copper redox reaction (2.1) or its step reactions (2.8a)–(2.8b).

An example composition of a typical microvia filling electrolyte is given in table 3.1. The additive components in table 3.1, except for the chloride ion, are various organic compounds and, therefore, given only characteristic names according to their function in the process. They are present in the electrolyte in very small concentrations and controlling these concentrations is essential to administrating the whole via filling process. Typically an operating range is given, within which the process operators try to maintain the concentration of each additive. If the operating limits are crossed, the product batch is discarded and re-produced after bath maintenance, which is costly. Online monitoring of the additive concentrations is difficult since, as said, their concentrations are very small and determining any of the concentrations usually requires for a bath sample to be analyzed in the laboratory. Online

measurements of bath additive concentrations are not known by the author.

	Electrolyte component	Concentration
Main components	$CuSO_4$	800 mol/m^3
	H_2SO_4	1000 mol/m^3
Additives	Cl^-	< 3 mol/m^3
	Suppressor Accelerator Leveler	< 1 mol/m^3

Table 3.1: One typical composition of a microvia fill electroplating electrolyte solution that is used in DC electroplating. The electrolyte composition can vary significantly between different via fill processes.

Several mechanisms, by which the additives modify the copper deposition process during via filling, have been proposed in the literature [e.g. 22–26]. The mechanisms outlined here are those that are chosen for examination in this thesis work and an overview of other variants is found in [6]. Though the typical components of the via fill additive chemistry are outlined below, significant challenges to the research of industrial via filling processes are brought by the fact that in practice, the microvia fill process chemistry is always proprietary. This means that only the process supplier knows exactly what chemicals go into the system. Indeed, the electrolyte bath recipe is with what the industrial process chemistry providers like Atotech, Enthone and Rohm&Haas make their profit on. Due to the diversity of the process chemistries, also the nomenclature related to the additives is *plentiful*, to say the least. The proprietary nature of the topic has had its effect, manifesting in several trade names appearing in the technology nomenclature. In this thesis the aim is to use a consistent terminology and, therefore, some additive names may differ from those in the original references, the meaning still being the same.

3.2.1 The main additive components

The additives found in copper electroplating baths that are applied in the manufacturing of PCBs and ICs can be divided into four categories: the chloride ion, suppressors, accelerators and levelers. Except for the chloride ion, the category names reflect the (net) effect that the additives have on the copper redox reaction (2.1).

The chloride ion

Chloride has for long been known to act as a catalyst for the copper reduction reaction [9, 27], and a mechanism for the catalyst effect is proposed in [28]. However, the most important role of the chloride additive in microvia filling baths is its interaction with the suppressor and accelerator additives [25, 29–33]. The chloride ions are provided by adding, e.g., HCl or NaCl to the solution. Typical chloride concentrations in commercial plating baths vary between ca. 1 mmol/l and 2.9 mmol/l (30-90 ppm) [34–36].

Suppressors

The suppressor additives are typically large-sized polymer compounds. One common suppressor is polyethylene glycol (PEG), with a molecular mass between 3 400 g/mol and 8 000 g/mol [33, 37]. The concentration of suppressor additives varies from 10 µmol/l to 100 µmol/l, typically being given in ppm[4] and being around 200 ppm [29, 35, 37]. The suppressor additives are added to the electrolyte by admixing appropriately diluted stock solutions.

The inhibition effect of the added polymer is based on it forming a complex compound with chloride [38]. Also the Cu^{+} ion is suggested to act as a linking ion in the complex [39–41]. The suppressor complex (polymer + Cl^{-} + Cu^{+}) then creates a blocking layer on the cathode, which physically stops access of the reducing Cu^{2+} species to the cathode surface [35, 37]. An illustration of the suppressor complex in effect (without the linking Cu^{+} ions shown), adopted from [33], is shown in figure 3.8. A recent review study of the polymer suppressors for copper electrodeposition is found in [42].

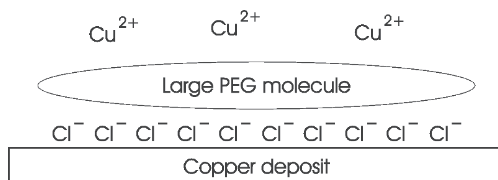

Figure 3.8: An illustration of how the large PEG polymer molecule in combination with chloride ions forms a blocking layer on the copper cathode surface [33].

[4] The corresponding molar concentration of the suppressor thus depends on its molecular weight.

Accelerators

The accelerator additives basically cancel the effect of the suppressing additives, by disrupting the suppressor layer that inhibits copper deposition, and thereby effectively accelerate the deposition process [43–45]. The accelerator chemicals are organic compounds that contain sulphur. Bis-(sodiumsulphopropyl) disulfide (SPS, 308 g/mol) or its derivative 3-mercaptopropane-1-sulfonic acid (MPSA, MPS, 155 g/mol) are unquestionably the most commonly applied and studied ones but also other options have been explored [46, 47]. Also the accelerator additives are present in the bath solution in micromolar concentrations, e.g., in the range of 0.1 to 10 µmol/l. However, studies show that it is not so much the absolute concentration of the accelerator, as it is the accelerator concentration relative to the chloride ion concentration that determines the eventual effect [30]. It has also been shown that the metal surface shape change has a strong influence on the local deposit growth velocity when accelerators are used [48–50]. This coupling between the microscale shape change of the metal surface and the local change in copper reduction rate is explained by the capability of the accelerator species to remain segregated on the copper surface and, therefore, to accumulate to those locations where the surface shrinkage is the greatest. Increased incorporation of accelerator into the copper deposit at areas where the surface shrinks the most has also been reported [51].

Levelers

Levelers are cyclic or heterocyclic nitrogen-containing compounds, significantly smaller in molecule size than the suppressors. Some examples of leveler additives include Janus Green B (JGB, 475 g/mol), thiourea (77 g/mol), benzotriazole (BTA, 119 g/mol), 2-aminobenzothiazole (2-ABT, 150 g/mol)) and polyethyleneimine (PEI) [52–55]. Also a generic leveler formulation for modeling purposes is given in [56]. The exact mechanism by which the levelers affect the copper deposition is not clear, and surely it depends on the chemical system. However, the suggested mechanisms for the leveler effects assume that the leveler chemical is a copper reduction inhibitor, just like the suppressor, and that the leveler can disrupt the accelerator effect on the copper surface due to its very strong adsorption capability [20, 53, 56]. Since the leveling mechanism is, in any case, a mechanism that includes interaction with other additives too, an isolated study of only the leveler effects is difficult to conduct. Clearly visible effects of the leveler reducing deposit overgrowth have, however, been reported for various leveler chemicals [53, 55]. Also computational models including a leveler system have been reported [56, 57].

In the via fill models documented in [P1, P2] there is no leveler compound included. This is because at the time when the models were created, there was no leveler

included in the target process either. It is noteworthy, however, that the formulation of the additive effects and their interactions in the models is very generic, which enables modifying and expanding them rather straightforwardly in future work.

3.3 Surface mass balance of the additives

Based on Sections 3.1 and 3.2, it is clear that, in order to model the microvia fill process, the interplay of the additive components on the copper metal surface must be somehow included in the model. In the end, it boils down to computing the *mass balance* of the additive chemicals on the copper surface. In the via fill models included in this thesis, it is assumed that the mass balance of surfactants is determined by the following distinct subprocesses:

- Adsorption and desorption of the additives to and from the copper surface
- Consumption of the surface-adsorbed surfactants on the metal surface, due to the surfactants either being buried into the copper deposit or being decomposed in a chemical reaction
- Local accumulation or decrease of the mass of such surfactants that are able to "float" on top of the deposited surface, when a curved surface is deposited
- Diffusion of surfactants along the surface, when a surface concentration gradient is exists

The consumption effect is considered to occur via both, (i) a preceding adsorption step (i.e., that the additive is first adsorbed on the surface and then consumed) and, (ii) directly from the electrolyte near the copper surface (i.e., without ever being adsorbed on the copper surface). Furthermore, not all additives need necessarily be influenced by all of the subprocesses listed above.

The amount of a surfactant effective on a part of the surface is described by the surface concentration, Γ (mol/m^2), of the surfactant. The surface concentration determines, e.g., how strong the inhibiting effect of a suppressor is. The magnitude of this effect can vary very significantly between different locations on a surface, depending on the surface shape, as well as on the system chemistry. The basis for computing the surface concentration in this thesis is the principle of mass conservation applied on the considered surface patch dA, with area $A(t)$ [58, 59]. The principle is formulated as the equation

$$\frac{d}{dt}\int_{A(t)} \Gamma dA = \int_{A(t)} \left(\frac{d\Gamma}{dt} dA + \Gamma \frac{d}{dt} dA\right) = 0. \tag{3.1}$$

As illustrated in [58], the integral form given in (3.1) can be derived to a differential equation for Γ on the evolving surface. Given that the movement velocity of the examined surface is $\mathbf{v}$,

$$\frac{\partial \Gamma}{\partial t} = -\nabla_T \cdot (\Gamma \mathbf{v}_T) - \Gamma (\nabla_T \cdot \mathbf{n}) (\mathbf{v} \cdot \mathbf{n}) . \tag{3.2}$$

In (3.2), the subscript symbol T denotes a tangential variable, i.e., $\mathbf{v}_T$ is the surface tangential velocity (m/s) and ∇_T is the tangential differential operator [P7]. $\mathbf{n}$ is the surface boundary outward normal vector.

No adsorption, desorption, diffusion etc. processes are yet considered in (3.2). Only the influence of the surface deformation on the local surface concentration of a surfactant readily attached on the surface is considered.

The meaning of the time derivative $\partial\Gamma/\partial t$ in (3.2) is further clarified in [60]. There it is concluded that the derivative in (3.2) is considered specifically for a surface moving normal to itself, which is the case in all physical processes. In practice, the surface movement velocity is always considered exactly as the surface movement normal to itself, but in numerical models this may not be so. Therefore, also the form

$$\frac{\partial \Gamma}{\partial t} = -\nabla_T \cdot (\Gamma \mathbf{v}_T) - \Gamma (\nabla_T \cdot \mathbf{n}) (\mathbf{v} \cdot \mathbf{n}) + \mathbf{v} \cdot \nabla_T \Gamma \tag{3.3}$$

is given in [60] for $\partial\Gamma/\partial t$, where the time derivative is now considered in the case of arbitrary surface movement. Equation (3.3) is also suitable for numerical modeling in the computational framework chosen in this thesis and, therefore, it is the starting point for the model formulation.

However, in [P7] (3.3) is still further simplified by noticing that

$$\nabla_T \cdot (\Gamma \mathbf{v}_T) = \nabla_T \Gamma \cdot \mathbf{v}_T + \Gamma(\nabla_T \cdot \mathbf{v}_T) \tag{3.4}$$

and that

$$\mathbf{v} \cdot \nabla_T \Gamma = \nabla_T \Gamma \cdot \mathbf{v}_T . \tag{3.5}$$

Substituting (3.4) and (3.5) in (3.3) the equation becomes

$$\frac{\partial \Gamma}{\partial t} = -\Gamma (\nabla_T \cdot \mathbf{v}_T) - \Gamma (\nabla_T \cdot \mathbf{n}) (\mathbf{v} \cdot \mathbf{n}) . \tag{3.6}$$

As discussed in [P7], (3.6) be reformulated to improve the computability of $\partial\Gamma/\partial t$ on boundaries that contain singularity points (i.e., on non-smooth boundaries). By using the identity

$$(\mathbf{I} - \mathbf{n}\mathbf{n}^{\mathsf{T}}) : \nabla \mathbf{v} = (\nabla_T \cdot \mathbf{n})(\mathbf{v} \cdot \mathbf{n}) + (\nabla_T \cdot \mathbf{v}_T), \tag{3.7}$$

can (3.6) be formulated as

$$\frac{\partial \Gamma}{\partial t} = -\Gamma(\mathbf{I} - \mathbf{n}\mathbf{n}^{\mathsf{T}}) : \nabla \mathbf{v}, \text{ where} \tag{3.8}$$

the colon (:) denotes a scalar product between the multiplied terms [P7eq. (19)]. Using $(\mathbf{I} - \mathbf{n}\mathbf{n}^{\mathsf{T}}) : \nabla \mathbf{v}$ in (3.8) has been shown to reduce numerical noise on a non-smooth boundary, compared to the equivalent computation carried out by using the terms $(\nabla_T \cdot \mathbf{v}_T)$ and $(\nabla_T \cdot \mathbf{n})$, included in 3.6, [P7, 2, and references therein].

As mentioned, none of the equations (3.2), (3.3), (3.6) or (3.8) contain terms for including the effects of other mass transport phenomena than those evoked by the surface movement. The surface diffusion term is already given in [58, 60, P7], and is included in the governing equation in the standard manner. Adding the surface diffusivity term to (3.6) yields

$$\frac{\partial \Gamma}{\partial t} = -\Gamma\left(\nabla_T \cdot \mathbf{v}_T\right) - \Gamma\left(\nabla_T \cdot \mathbf{n}\right)\left(\mathbf{v} \cdot \mathbf{n}\right) + D_s \nabla_T^2 \Gamma, \text{ where} \tag{3.9}$$

D_s is the surface diffusivity (m^2/s) of the surface-adsorbed surfactant. The effect of the surfactant surface diffusivity on the via fill process in both nanometer and micrometer scale is discussed in [2, 61, P7]

The rest of the mass transport phenomena, namely adsorption, desorption and consumption are added to the governing equation as source terms.

$$\frac{\partial \Gamma}{\partial t} = -\Gamma\left(\nabla_T \cdot \mathbf{v}_T\right) - \Gamma\left(\nabla_T \cdot \mathbf{n}\right)\left(\mathbf{v} \cdot \mathbf{n}\right) + D_s \nabla_T^2 \Gamma + N^{ads} - N^{des} - N^{cons} \tag{3.10}$$

In (3.10), N^{ads}, N^{des} and N^{cons} are the additive mass fluxes corresponding to the adsorption, desorption and consumption ($mol/m^2/s$) of the additive, respectively. Equation (3.10), therefore, enables solving the local time differential of Γ on an evolving surface as a function of the affecting mass fluxes as well as the local surface velocity and geometry change, i.e., to compute the *mass balance* of Γ. Figure 3.9 illustrates the factors that affect the surfactant surface concentration on a deforming, non-planar surface.

The generic and separated formulation of the mass fluxes related to adsorption (N^{ads}), desorption (N^{des}) and consumption (N^{cons}) in (3.10) clarify the physical content of the equation and simplify its computational implementation. However, finding the equations for these fluxes, and the parameters that affect them is again another important task in building a microvia fill model. Some candidates for these fluxes are given in, e.g., [P1, P2]. A short discussion related to this subject is also given below, in Sections 3.3.1 and 3.3.2.

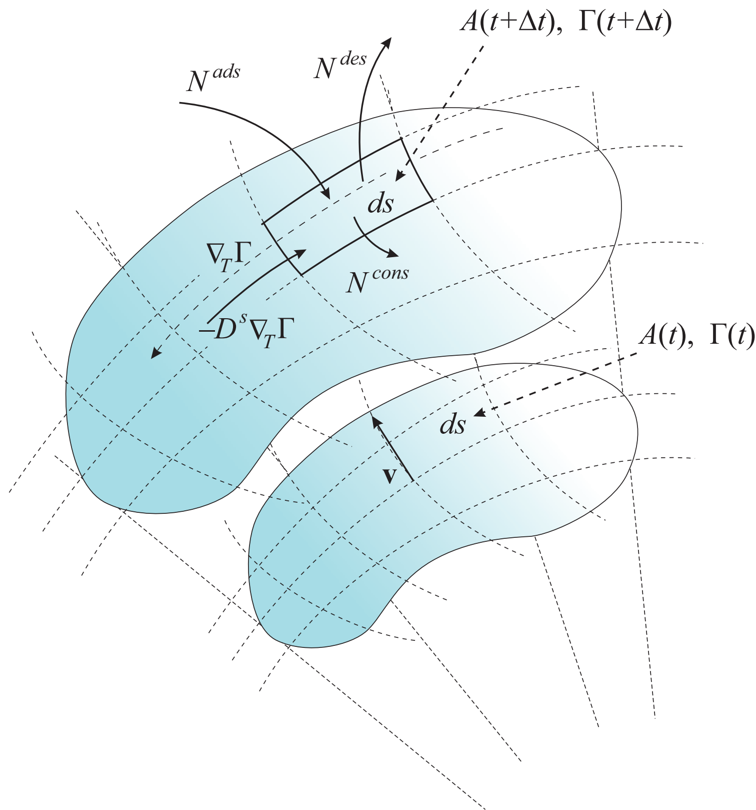

Figure 3.9: Different factors that are considered to affect the surfactant surface concentration on an evolving surface (surfactant mass fluxes are denoted by curved, solid-line arrows). Picture originally published in [2].

It should be noted that the formulation for $\partial\Gamma/\partial t$ given in [P1, P2, P8] is somewhat different from the equations presented above. This is mainly because the surfactant mass balance formulation was developed in several steps over time and thoroughly clarified only in [P7], which is the latest of the articles included in this thesis. The main ideas behind the equations, however, remain the same.

3.3.1 Adsorption and desorption of surfactants

The chemical mechanisms through which the via fill additives adsorb on and desorb from the copper surface have only recently begun to unveil themselves, through extensive experimental examination of the system. Therefore, early models rely on various mechanisms from fast, irreversible first order adsorption (simple) [22] to an adsorption-desorption balance of arbitrary order (complex) [57]. The parameters for the models are found, at least partially, by fitting the model output with

measurement data. At present, as the real complexity of the process is gradually discovered, a standard reaction mechanism of competitive adsorption of additives, complemented with desorption, seems to be the mechanism that most adequately describes the experimental results. It also provides a viable tool for computational simulation [e.g., 57, 62]. A similar approach is utilized also in this thesis.

In [P1, P2], the adsorption-desorption balance of the additives is described with a simple first order system. In these, the accelerator additive may adsorb onto a site on the copper surface where a suppressor additive already has adsorbed, but the opposite is not possible [e.g., 63]. Therefore the adsorption and desorption fluxes, N_i^{ads} and N_i^{des} (mol/m^2/s) become,

$$N_{Supp}^{ads} - N_{Supp}^{des} = k_{Supp}^{ads} c_{Supp} (\Gamma_{Supp}^{sat} - \Gamma_{Supp} - \frac{\Gamma_{Supp}^{sat}}{\Gamma_{Acc}^{sat}} \Gamma_{Acc}) - k_{Supp}^{des} \Gamma_{Supp} \tag{3.11}$$

for the suppressor and

$$N_{Acc}^{ads} - N_{Acc}^{des} = k_{Acc}^{ads} c_{Acc} (\Gamma_{Acc}^{sat} - \Gamma_{Acc}) - k_{Acc}^{des} \Gamma_{Acc} \tag{3.12}$$

for the accelerator [P1, eq. (14)-(16), P2, eq. (9)-(10)]. In (3.11) and (3.12), Γ_i^{sat} stand for the saturation surface concentration (mol/m^2) of the adsorbing species and k_i^{ads}, k_i^{des} are the rate coefficients for adsorption and desorption (m^3/mol/s, 1/s), respectively.

The difference between the model documented in [P1] and in [P2] is that in the former, the adsorption-desorption balance is assumed fast and, therefore, always in steady-state. This enables solving a static equation for the surface concentrations of the additives [P1, eq. (24) and (20)]. In [P2], then again, the adsorption and desorption processes are modeled dynamically, without the steady-state assumption, which yields a first order ordinary differential equation to be solved at the cathode boundary for the surface concentration of each additive [P2, eq. (8)].

The focus of experimental study related to the adsorption-desorption balance of the additives was first in the dynamics of the interrelated adsorption and desorption processes. The aim was to find appropriate constant parameters for the first order adsorption-desorption processes. Several time-scales for the processes have been found, the relevant transient times ranging from less than a second to over 1000 seconds [23, 36, 64, 65]. In an effort to keep the system simple, constant rates for adsorption and desorption have been the general starting point, but recently adsorption and/or desorption of all additives (Cl^--suppressor complex, the accelerator, and the leveler) have been found to be dependent on the cathode potential [32, 66–68]. If this feature is to be included in a microvia fill electrolysis system model, it means that a model structure that takes into account all the potential components in the system (shown in (2.6), (2.3)) and incorporates the effect of changes in $\Delta\phi_e$ into

the k_i^{ads} and k_i^{des} coefficients should be constructed. The model structure shown in, e.g., [P4] may be utilized for this.

3.3.2 Consumption of surfactants

Once adsorbed on the electrolyte surface, the electrolyte additives may either remain "floating" on the surface [45, 66], or get consumed on the surface due to inclusion into the deposit [36, 51, 54, 69, 70] or (electro)chemical decomposition [32, 36, 71, 72]. For instance, chloride is known to precipitate as CuCl, and in suitable conditions, CuCl crystals can be observed to accumulate on top of electroplated microvias [30, 73]. An important decomposition mechanism of the additives is their oxidation, especially in baths where air agitation is used to stimulate electrolyte flow on the cathode. Though additive oxidation has been pointed out as a special problem of systems with inert anodes [16, 74], chemical decomposition of the additives creates by-products, which generally are harmful to the whole process and, therefore, need to be filtered out. Though it has been shown that inclusion of the additive chemicals into the deposit does occur, the best explanations for bottom-up fill of vias are provided by the models, which assume that at least the accelerator remains segregated on the cathode surface [56, 57, P2]. It is likely that both phenomena do occur concurrently. However, also models assuming that the consumption or incorporation of the inhibiting or leveling agents during deposition is negligible or low have been reported [23, 54, 75].

In [P1, P2], additive consumption is considered to occur through a first order chemical reaction dependent on the concentration of the additive at the electrode surface, though in [P1], the consumption of the accelerator additive is considered minimal and is, therefore, neglected. The consumption flux is calculated as $N_i^{cons} = k_i^{cons} c_i$, where N_i^{cons} is the mass flux (mol/m^2) corresponding to the additive consumption reaction and k_i^{cons} the consumption reaction rate coefficient (m/s) [P1, eq. (21), P2, eq. (7)].

3.4 Computational modeling of microvia filling

The computational models of electrochemical feature filling processes found in the literature focus on describing the process in one isolated via or trench, on an isolated electrode surface. The first models that can be counted into this group are from the 1990's [22, 76] and describe the copper electrodeposit growth in sub-micron features. Back then, the superconformal growth of the modeled copper deposit was obtained through a mechanism of diffusion limited mass transfer of the suppressor

additive. Gradually, as more knowledge of the chemical processes behind superconformal copper deposition was gained, the accelerator effects were added [49, 63] to the models. Introducing the accelerator effects produced the curvature enhanced accelerator coverage (CEAC) model, reviewed in [24]. The CEAC model still remains as the generally accepted approach for modeling the feature filling processes, especially for sub-micron features. However, also the leveler effects are included in the most recent models [56, 57]. Some models exist that include more than one feature [77, 78]. What should still be noted, is that all the models mentioned here discuss the feature filling process in the context of IC manufacturing, i.e., in submicron scale. There are some differences between the systems that also affect how they should be modeled and, e.g., the relevance of the CEAC effect with respect to the feature size has been considered in [2, 79]. Despite several studies are mentioned above, the reports of actual *microvia fill* models remain few, and as far as the author knows, the first models are documented in [P1, P2].

One more important characteristic of the feature filling processes is that the phenomena that are simultaneously relevant in the process occur in both the macro scale, as well as in the microscopic scale. In terms of computational modeling this means that in order to build a system model of the microvia fill process, phenomena that actually span over eight to ten orders of magnitude in both scales of time and length need to be incorporated into one model. This presents a multiscale modeling problem [80, 81] and instead of directly including all the phenomena in one huge model, the means for implementing such multiscale models need to be thought over. One such multiscale modeling technique for including the macro-scale electric field effects is presented in [P4].

The shape change of the model domain geometry is clearly inherent in via fill process models. Since the governing equations are partial differential equations in time and space, the model geometry shape change must be accounted for, in order to keep the solutions sensible. In the models described in this thesis, the Arbitrary Lagrange-Eulerian (ALE) method was chosen as the computational method to capture the shape change of the model geometry. The ALE method was chosen due to the simplicity of its application, the analytical transparency of the method, and due to the plentiful readily available documentation about the method. Furthermore, and perhaps most importantly, the ALE method was found to enable modeling the necessary shape change processes at a very reasonable computational cost, making the model development work fast.

Other well-established methods applied for similar shape change problems are the Monte-Carlo (MC) method [82–86] and the level-set method, which seems to have been developed somewhat concurrently with the problem domain discussed in this thesis [50, 87, 88]. Though not detailed here, both of these methods have their undisputed benefits compared to the ALE method. However, both of them are

also computationally significantly heavier than the ALE method (when comparable accuracy is desired). For instance, the MC computation of one (nano)via filling experiment typically takes from one to three days on an up-to-date computer [89] and similar computation times may be expected with the level-set method too [50]. Developing model-based control systems based on such models or methods that require enormous computational efforts is not sensible. Consequently, simplified and computationally significantly faster versions of the mentioned models have been developed [90, 91] and also the ALE-based models developed in this thesis are typically solved within tens of seconds or within minutes on a regular desktop PC. A variety of ad-hoc computational methods to simulate the propagating copper front during electrodeposition has also been developed for the early models of copper electrodeposition in sub-micron features [22, 49, 76, 92–94].

3.4.1 The ALE method as applied in this thesis

Only a brief review of the ALE method and its utilization in the models of this thesis is given here. For the interested reader, more information about the ALE method is found in [95, 96].

The ALE method enables formulating the differential equations of a deforming system in such a way that they can be solved in a referential system which appears fixed to the solver software. The basic principle is to use one set of coordinates, $\mathbf{x} = (x, y)$, for the deformed domain $\Omega_{\mathbf{x}}$, and another, $\mathbf{X} = (X, Y)$, for the referential domain $\Omega_{\mathbf{X}}$. Only two coordinates are given for each coordinate system, since the actual microvia fill computer models are created in only two dimensions. The simplification of the system geometry can be done thanks to the axial symmetry of the microvia or the plane-symmetry of a microtrench. Here, the x and X symbols correspond to the horizontal coordinates and the y and Y corresponding to the vertical coordinates of a two-dimensional, Cartesian or axially symmetric cylindrical coordinate system[5].

A mapping between the two coordinate systems is obtained with the deformation gradient $\mathbf{F}$, where $\mathbf{F} = \partial\mathbf{x}/\partial\mathbf{X}$. If the deformation process is considered only over a short time period at a time, the deformations $\partial\mathbf{x}/\partial\mathbf{X}$ may be considered to be small enough, so that approximating the differentials with differences stays sufficiently accurate. Then by considering $\mathbf{x}$ as a (static) function of $\mathbf{X}$ at each time step (i.e., $x = x(X, Y)$ and $y = y(X, Y)$) and applying the chain rule on the differential $d\mathbf{x}/d\mathbf{X}$,

[5] The x, y-based coordinate names are used for simplicity and to avoid symbols overlapping with r, R and z.

the differential can be rearranged as

$$\begin{bmatrix} dx \\ dy \end{bmatrix} = \mathbf{F} \begin{bmatrix} dX \\ dY \end{bmatrix} = \begin{bmatrix} \frac{\partial x}{\partial X} & \frac{\partial x}{\partial Y} \\ \frac{\partial y}{\partial X} & \frac{\partial y}{\partial Y} \end{bmatrix} \begin{bmatrix} dX \\ dY \end{bmatrix}, \tag{3.13}$$

[P2, eq. (13)-(14), P7 Section 2.1]. Then, by tracking the deformation gradient over each time step, the model deformation can be followed even in a time-dependent model, where the deformation occurs over a significant amount of time and is (nearly) arbitrary.

The transformation (3.13) gives the relation between differentials (or differences) in the deforming and referential coordinate systems. The transformation is obtained, as said, by considering $x = x(X, Y)$ and $y = y(X, Y)$, and taking the differentials dx/dX (or dx/dY) and dy/dX (or dy/dY), separating variables (with respect to dX and dY) and collecting the terms into a matrix. For example, applying the chain rule we obtain that

$$\frac{dx(X,Y)}{dX} = \frac{\partial x(X,Y)}{\partial X}\frac{dX}{dX} + \frac{\partial x(X,Y)}{\partial Y}\frac{dY}{dX} \tag{3.14}$$

and by separating the variables dx and dX,

$$dx(X,Y) = \frac{\partial x(X,Y)}{\partial X} dX + \frac{\partial x(X,Y)}{\partial Y} dY. \tag{3.15}$$

Doing this also for the other elements and arranging them into matrix form yields (3.13).

In the computational model, the domain $\Omega_{\mathbf{x}}$ is represented by the deformed mesh, and its node points, and similarly the domain $\Omega_{\mathbf{X}}$ is represented by the fixed mesh and its node points. An illustration of these is given in figure 3.10.

The practical application of the ALE method happens by formulating the governing equations first in the deforming system and then transforming the equations to the referential system, where they can be solved. This *back-transformation* is obtained by using the inverse $\mathbf{F}^{-1}$. That is, all the differentials in the deformed system are formulated as differentials in the referential system by using the elements in $\mathbf{F}^{-1}$. For example, by using matrix notation the spatial differentials of a scalar variable f are transformed so that the gradient in the deformed coordinates is

$$\nabla_{\mathbf{x}} f = (\mathbf{F}^{-1})^{\mathsf{T}} \nabla_{\mathbf{X}} f, \text{ where} \tag{3.16}$$

$\nabla_{\mathbf{X}} f$ denotes the gradient in the referential system. The transpose is included in (3.16) the gradient vectors are considered in this thesis to be column vectors. Therefore, the eventual form of the ale-transformed equations depends on the vector definition and, if the gradient were a row vector we would have $\nabla_{\mathbf{x}} f = \nabla_{\mathbf{X}} f \mathbf{F}^{-1}$.

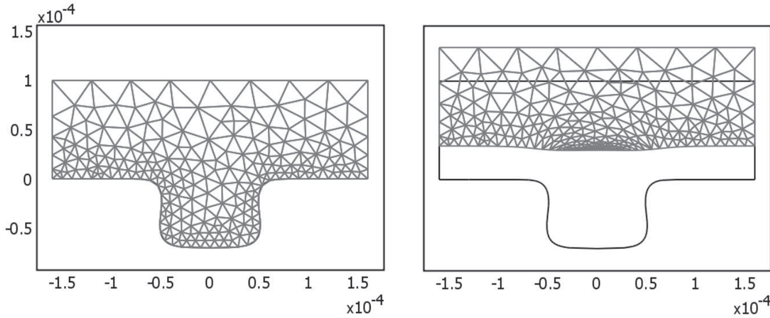

Figure 3.10: The computational mesh of the microvia fill model at the initial time (left) and in the end of the simulation (right). The deformed mesh, representing $\Omega_{\mathbf{x}}$ is shown in the figure, but the mesh representing the referential domain, $\Omega_{\mathbf{X}}$, is equal to the deforming mesh at the initialization of the computation, shown on the left.

After the equations are formulated in the referential system, they are solved and the shift $\mathbf{x} - \mathbf{X}$, corresponding to the mesh displacement, is applied to the mesh and the plot points during the post processing phase. Several readily ALE-transformed continuum equations are found in the literature, e.g., in [96], though their computational implementation is not specified there.

When utilizing the finite element method to solve partial differential equations, as in the thesis models, the equations are essentially solved in their variational form - or integral form. To maintain the physical consistency of the ALE-transformed integral equations during their numerical solution, the infinitesimal volume element (i.e., the area element in 2D) also needs to be scaled appropriately. The scaling factor is obtained as the determinant $\det(\mathbf{F})$. The same applies on the model boundaries, where the infinitesimal area element (line element in 2D models) needs to be scaled [P7eq. (16)]. Details of formulating the equations and computing the solutions for the ALE-transformed boundary variables are given in [P7].

Physically, the shape change of the microvia model domain is caused by the continuous evolution of the copper deposit surface. The actual movement, therefore, only occurs on a boundary, but to keep the computational model functional, all the mesh nodes in the model are relocated at each deformation step. So-called Laplace smoothing is applied in the thesis models to relocate the mesh nodes evenly over the model domain but also other methods for mesh point relocation have been presented [4, 97, 98].

The Laplace smoothing method used in the thesis is based on simply solving the stationary Laplace equation (3.17) for the mesh velocity $\mathbf{v}$ (m/s) at each time step of model simulation, with the appropriate boundary velocity conditions [P1, eq. (35),

P2, eq. (11)-(12), P7, eq. (1)].

$$\begin{cases} \nabla^2 \mathbf{v} = 0 & \text{in } \Omega_{\mathbf{x}} \\ \mathbf{v} = \mathbf{v}_{\partial\Omega_{\mathbf{x}}} & \text{on } \partial\Omega_{\mathbf{x}} \end{cases} \tag{3.17}$$

In (3.17), $\partial\Omega_{\mathbf{x}}$ represents the boundaries of the model domain $\Omega_{\mathbf{x}}$ and the spatial differentials of $\mathbf{v}$ are computed with respect to the reference coordinate system. The boundary conditions are obtained from the physical properties of the microvia fill copper deposition process. As the plating current density i_e is given on the boundary representing the deposited copper surface, the boundary normal velocity magnitude

$$\mathbf{v}_{\partial\Omega_{\mathbf{x}}} \cdot \mathbf{n} = i_e \frac{M_{\mathrm{Cu}}}{z_{\mathrm{Cu}} F \rho_{\mathrm{Cu}}}, \tag{3.18}$$

where M_{Cu} is the atomic mass of copper (0.06355 kg/mol) and ρ_{Cu} is the density of metallic copper (8960 kg/m^3). Note also that, since $\mathbf{v}$ is a vector with two elements, equation system (3.17) must in practice be considered as a system of more than two equations. The gradient $\nabla\mathbf{v}$ is not sensible without further interpretation, which in this case means considering the gradients of the components of $\mathbf{v}$ separately.

To eventually obtain the mesh point locations of the deformed mesh, the mesh velocity $\mathbf{v}$ is integrated in time, with the initial condition being $\mathbf{x} = \mathbf{X}$.

Nowadays, the ALE method is found as a built-in feature in the COMSOL computation software and, therefore, one does not necessarily need to implement the entire ALE configuration manually anymore when using COMSOL. However, understanding more of the ALE method than what is visible at the user interface of solver software, is ultimately necessary to ensure that the ALE method is applicable to the problem and that the solution is accurate. Furthermore, the built-in tools given with COMSOL for configuring ALE-based models do not allow for surface mass balance systems, such as (3.10) to be configured. Enabling the flexible configuration of the ALE method as well as the various boundary variables required by the surface mass balance system was also one of the reasons for utilizing the weak-form equation formulations, described next.

3.4.2 Weak formulations

The governing equations of the microvia fill models were formulated and configured to the COMSOL PDE solver in the weak form. The weak form is one kind of a variational form of the initial problem and the formulation is characteristic to the finite element method [99]. Using the weak form formulations increases the flexibility in configuring the equations for numerical solution and enables solving

the system without requiring the second order spatial differentials of the governing equation variables. The flexibility provided by the weak form configuration is necessary especially for solving boundary variables, such as the surface coverage and the surface concentration [P2, eq. (15), P7, eq. (7)-(9)]. The formulation procedure of weak form equations is in the context of this thesis rather mechanical, though it is somewhat affected by the usage of the ALE method. The mechanism is illustrated below and the Laplace equation in (3.17) is used as an example to describe the steps included in the procedure that was used.

1. Multiply the initial equation with a test function[6]. Here the test function is denoted by $\hat{\mathbf{v}}$.
$$\hat{\mathbf{v}}\nabla^2\mathbf{v} = 0$$
2. Integrate the equation over the considered domain $\Omega_{\mathbf{x}}$. As $\Omega_{\mathbf{x}}$ in our case is a 2D domain, i.e., an area, $dA_{\mathbf{x}}$ is used to denote the infinitesimal area element, where $dA_{\mathbf{x}} = \det(\mathbf{F})dA_{\mathbf{X}}$. Similarly, $ds_{\mathbf{x}}$ is used below (in step 4) to denote the infinitesimal line element on the boundary $\partial\Omega_{\mathbf{x}}$, which in this case is a curve. $ds_{\mathbf{x}}$ is obtained by using [P7, eq. (19)].
$$\int_{\Omega_{\mathbf{x}}} \hat{\mathbf{v}}\nabla^2\mathbf{v}dA_{\mathbf{x}} = 0$$
3. Reformulate the term to get rid of the divergence of the gradient[7].
$$\int_{\Omega_{\mathbf{x}}} \nabla\cdot(\hat{\mathbf{v}}\nabla\mathbf{v}) - \nabla\hat{\mathbf{v}}\cdot\nabla\mathbf{v}dA_{\mathbf{x}} = 0$$
4. Use the divergence theorem to reformulate the system.
$$\int_{\partial\Omega_{\mathbf{x}}} \mathbf{n}\cdot(\hat{\mathbf{v}}\nabla\mathbf{v})ds_{\mathbf{x}} - \int_{\Omega_{\mathbf{x}}} \nabla\hat{\mathbf{v}}\cdot\nabla\mathbf{v}dA_{\mathbf{x}} = 0$$
5. The integral on the boundary $\partial\Omega_{\mathbf{x}}$ is in many cases zero due to constraints but when it is non-zero, it is included in the model boundary conditions. Therefore, the term is omitted from the equation formulation for $\Omega_{\mathbf{x}}$ and what is left is
$$-\int_{\Omega_{\mathbf{x}}} \nabla\hat{\mathbf{v}}\cdot\nabla\mathbf{v}dA_{\mathbf{x}} = 0.$$

The last equation is the weak form of $\nabla^2\mathbf{v} = 0$ in $\Omega_{\mathbf{x}}$, as considered in the context of this thesis. After the reformulation, it is straightforward to apply the ALE transformations on the differentials in this equation and input it to the PDE solver.

[6] See, e.g., [99] for more information on the test function.

[7] The reformulation is based on using the rule $\nabla\cdot(f\mathbf{G}) = \nabla f\cdot\mathbf{G} + f\nabla\cdot\mathbf{G}$, where f is scalar and $\mathbf{G}$ vector-valued.

3.4.3 Microvia fill model output

The via fill models documented in [P1, P2] enable examining the copper electrodeposition process in the microvia domain under various conditions. The models produce information of several unmeasurable processes in the microvia fill system but, naturally, only measurable processes may be utilized to determine model parameters and to validate the models. Figure 3.11 shows the estimated and measured growth of the copper deposit in the center of the microvia bottom and on the level board surface during the electrodeposition process. The measured plot in 3.11 has been produced by plating microvias for a series of times, cross-sectioning the filled microvia samples and measuring the necessary dimensions from SEM-photographs. The photographs that show the microvia profile at various time instants are given in 3.12 and the corresponding estimate for the via profile evolution in 3.13.

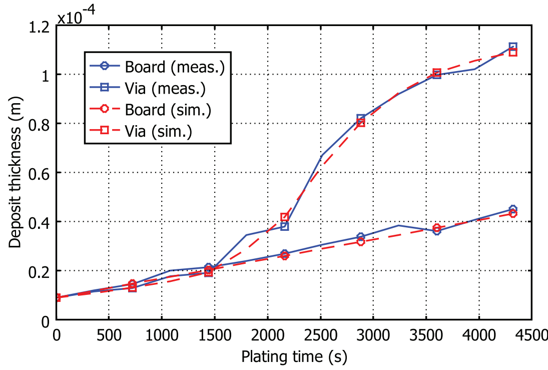

Figure 3.11: The thickness of the copper deposit inside the via (▫) and on the board surface (◦) plotted versus time. The dashed red line shows the estimate given by the model and the solid blue line is the corresponding measurement data. [P2]

3.5 Microvia fill process control simulation

The process control of industrial via fill processes is still mainly carried out by human operators. As described in Section 3.2, the control operations are mainly monitoring the electrolyte composition and keeping it within certain prescribed bounds. The plating machinery is used only for starting and stopping the plating process at given time instants and for keeping the cathode current density at a desired level.

Some model-based methods to control feature filling have been suggested for the

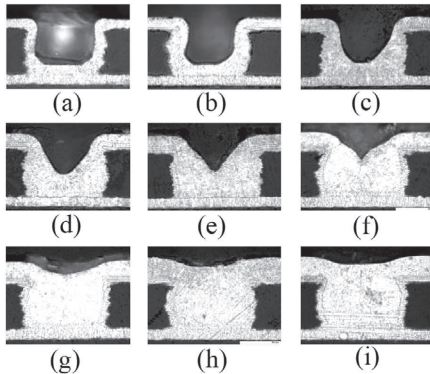

Figure 3.12: Cross-section images of microvias filled in via-fill experiments. Fill times are (a) 12, (b) 18, (c) 24, (d) 30, (e) 36, (f) 42, (g) 48, (h) 54, and (i) 60 min. The via diameter is approximately 100 µm and the substrate thickness is 65 µm. [P2]

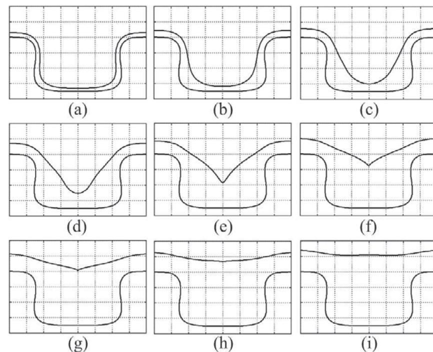

Figure 3.13: Microvia cross-section profiles estimated by the model. Simulation times are (a) 12, (b) 18, (c) 24, (d) 30, (e) 36, (f) 42, (g) 48, (h) 54, and (i) 60 min. The via diameter is 100 µm and the substrate thickness is 70 µm. [P2]

sub-micron scale processes, but these are mainly model-based estimates for preconfiguring the process chemistry so that unwanted outcomes are avoided [16, 57, 100–102]. The control methods presented in this thesis are intended for online control or optimization of the via fill process. In the thesis, two possible control strategies, whose design and examination is enabled by a validated microvia fill process model, are proposed and investigated in the thesis work [P5, P6, P9].

The first strategy, given in [P9], is aimed at predicting the end-time t_{end} (s) of the via fill electroplating process, when a certain end-time via fill ratio r_{end} is desired. The idea is to control the electroplating bath power source output voltage so that a linear growth of the via fill ratio $r(t)$ is obtained. As the via fill ratio growth is linear, $dr(t)/dt = b$, where b is constant. It is then straightforward to predict the time when the via fill ratio reaches the desired value r_{end}. The cost function J_1^u [P9, eq. (7)] for this control can be simply formulated as

$$J_1^u = \left[r(t)H + r(t)h_B(t) - h_V(t)\right]^2 , \tag{3.19}$$

where H is the via hole depth (m) and $h_B(t)$,$h_V(t)$ are the deposit thickness on the level board surface and in the via, respectively. The function J_1^u is then minimized at each time-instant ($t \geq 0$) during the simulation and the simulation is run until the computed end-time, $t_{end} = r_{end}/b$.

The study reported in [P9] outlines the principles by which via fill control ultimately should be conducted. In practice, there is no possibility of controlling the chemical

parameters of the via fill process (i.e., the concentration of the chemicals). Therefore, via fill process control should be implemented by manipulating the electrical variables (i.e., the cathode current density and the cell voltage) and the plating time. It is shown in [P9] that actually rather significant changes in the electrode surface overpotential values are required to obtain the desired control, and that rather small changes in the cell voltage are sufficient to produce the desired process changes. However, the approximations used for cell ohmic loss in [P9] are very rough, which makes the practical applicability of the system as such questionable but by, e.g., utilizing the model structure developed in [P4] the control system can be improved.

The second control strategy developed in [P5, P6] aims for actually optimizing the microvia fill process operation, under given manufacturing preferences. The goal is to simultaneously seek for the optimal cathode current density and plating time, when the process operation cost is given in terms of two practical variables, the process output quality and the process lead time. Process output quality is measured with the thickness of the copper deposit on the level board surface and typically, a thin copper deposit on the board surface is desired. Process lead time is measured directly with the plating time.

There is a tradeoff between the two cost variables. If a thin deposit on the board surface is desired, one should apply a low cathode current density. However, if a short lead time is desired, the plating current density should be high for the microvia to fill swiftly. Furthermore, a high plating current density easily leads to the depletion of Cu^{2+} ions on the cathode, especially inside the via, thus creating a brittle (*burnt*) deposit and further reducing process output quality.

Equation (3.20) [P5, eq. (2)] represents the control cost function J_2^u, with r_{end} when a constant average plating current density i_{target} (A/m^2) is used throughout the plating. This corresponds to the situation in the manufacturing line too. k_1 and k_2 are weight parameters that enable incorporating the production preferences into the cost function – k_1 is used to punish for deposit growth on the board surface and k_2 for a long process duration.

$$J_2^u = \left[r_{end}(H + h_B(t_{end})) - h_V(t_{end})\right]^2 + k_1 h_B^2(t_{end}) + k_2 t_{end}^2 \qquad (3.20)$$

Given the parameters r_{end}, k_1 and k_2, the cost J_2^u is then minimized by modifying the modeled plating time, t_{end}, and plating current density, i_{target}, which both can also be adjusted by the process operator. The deposit growth values h_B and h_V are computed with the microvia fill model, but in order to account for the problem caused by the depletion of Cu^{2+} ions on the cathode, the values of i_{target} are limited so that no depletion occurs.

The optimal controls (t_{end}, i_{target}) in various cases of manufacturing preferences are found by using both, the gradient descent method and an exhaustive search method. A gradient descent algorithm finds the near-optimum values for the control with only a few iterations. But due to the shape of the cost function, it takes several iterations more for the method to locate the actual optimum values. The exhaustive search enables visualizing the cost function and it soon becomes obvious that the cost function forms an *optimum valley*, shown in figure 3.14. Though the valley has a global optimum, the valley bottom is rather flat, which slows down the optimization based on the gradient descent method. Also an example of the optimal controls computed with the exhaustive search method, in four different cases of manufacturing preferences (detailed in [P5]) is shown in figure 3.14.

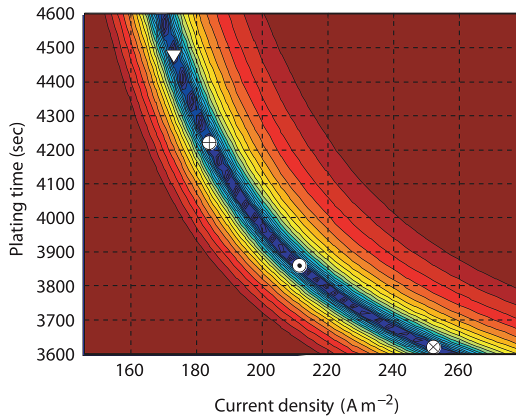

Figure 3.14: The cost function and the optimal values for cathode current density and plating time in four different cases of manufacturing preferences. The optimal values are indicated by the four points on the bottom of the *optimal cost valley* (dark blue). The color indicates the cost and the cost value is shown on a logarithmic scale. All values over log 5 are colored in uniform dark red. [P5]

The control strategy is, in this case too, implemented by controlling the cell voltage and by lifting the boards out from the bath at the right moment. Therefore, the same problem related to estimating the cell ohmic loss, as included in the control system described in [P9], is inherent in the later control system too. The model structure developed in [P4] is meant for addressing this problem exactly.

4 Summary of the thesis

The work for this thesis was carried out in the ambitious attempt to develop a practical model-based control system for the microvia fill process. The majority of the work focused on developing the microvia fill process models, but a significant effort was also made in resolving problems related the computational techniques applied in the models. Especially implementing the surfactant mass balance computation required a considerable amount of time and energy.

Two microvia fill process models for one isolated microvia were developed in [P1, P2, P8]. This part includes a thorough study of the chemistry of the microvia filling process, several via filling experiments as well as the computational implementation of the microvia electroplating models by using the FEM-ALE framework. The equations presented in Sections 2.2 and 3 are brought into use in these models and the models are parameterized against practical data.

Most of the microvia fill process modeling work was based on literature studies and experimentation with the models, but without a notable amount of practical via filling experiments, the models could never have been completed. The experiments play an essential role also in the study of the copper electrolysis system, which was completed to support the via fill modeling work. Though, again, much of the mechanistic study was done based on the existing literature, the voltammetric experiments carried out in the Control Engineering Group facilities laid the foundation for parameterizing and validating the computer models. The only parts of the work that are not based on practical measurement data are the development of the microvia fill process control strategies and the analysis of the surface mass balance computation with the ALE method. Trying out the former in practice was not possible at the time being and the latter is, by nature, a computational and theoretical piece of work.

To support the study of additive effects on the copper reduction reaction, a copper electrolysis model was created in [P3] based on the elementary step-reactions of the copper redox system. The model also includes the effects of the copper disproportionation/comproportionation system as well as the dynamics of the copper sulfate dissolution reaction. The model enables exact examination of what effects do the reaction rates of the individual step reactions have on the copper electrode current density. It is these reaction rates that are influenced by the electrolyte additives in the microvia fill bath and the model, therefore, provides a tool for analyzing the mechanisms of the additive effects.

To enable expanding the microvia fill models developed in [P1, P2] to an electrol-

ysis cell model, a model structure that enables including the effect of the ohmic potential loss occurring in the cell bulk electrolyte into the model was developed in [P4]. A function to estimate the cell ohmic loss based on the cell geometry and the cell current is created by utilizing a 3D electric field model of a special-purpose electrolysis cell. The ohmic loss estimate and the equations given in 2.2 were then incorporated into a single system of equations, from which the electrode overpotential for one electrode is solved. The model yields the relevant electric properties of the electrolysis cell, e.g., the electrode overpotentials and current densities, based on only one input variable, the cell power source output.

In order to create and to understand the functioning of the models in [P1, P2], the implementation of the surfactant mass balance computation within the FEM-ALE framework was clarified in [P7]. The equations given in Section 3.3 and 3.4 were analyzed independently of the via fill system, the instabilities possibly harmful to the computational system are pointed out by simulations, and a technique to circumvent such instabilities is presented.

Finally two strategies for model-based control of the microvia fill process were developed and analyzed in [P5, P6, P9]. The principles of how model-based microvia fill process control can and should be carried out in practice were outlined and tried with extensive simulations.

In order to realize the described models, a good amount of research work was done to obtain numerical values for various parameters. This included, not only examining empirical data, but also developing estimator functions for various physical and chemical variables included in the model.

In summary, significant progress towards the ultimate aim of the work was reached through the development of a collection of the elementary components necessary to the desired control system. The main results of this thesis are summarized below.

4.1 The main results

The microvia fill models are the main result of this thesis. The models were calibrated with experimental data and found to yield reasonable results. The models provide information of several non-measurable process variables, such as the surface coverage of the additives and the copper ion concentration profile inside the via during deposition. Thanks to the computational methods applied to implement these models, they are comparable in accuracy, yet essentially lighter to compute than other similar models found in the literature. This is important when keeping

the design of model-based control systems in mind.

Further utilization of the microvia fill models described above and in [P1, P2] would be difficult, without further examining the underlying principles of copper electrolysis. Therefore, also the copper electrolysis model in [P3] and the electrolysis cell model structure given in [P4] also form an essential part of the thesis results. The models offer information from a significant number of such processes that by conventional means of experiments and measuring are left unexplored. For example, the model structure documented in [P4] enables simulating what effects the physical geometry of the microvia fill apparatus has on the system potential components. Doing such trials with practical, industrial environment would certainly be costly. Furthermore, the model structure given in [P4] enables also estimating the electrode (over)potentials, which normally need to be measured by utilizing a reference potential device. Such a reference device, however, is rarely available in practical industrial electrolysis systems because they are prone to break or wear out. The model provides information of all the cell potential components (given in (2.6)). By applying this model structure in the microvia fill process models, they can also be modified to better correspond to the actual, industrial microvia fill equipment.

Clarifying and analyzing the computational techniques related to implementing the surfactant mass balance computation on a deforming surface in models that are implemented in the FEM-ALE framework is a result as such. This result provides means to further improve the accuracy and computability of the microvia fill models developed in this thesis.

The simulation of the two numerically implemented microvia fill process control systems demonstrates the usability of the underlying strategies. The development of a complex control system is always started off with simulations and these simulations show that the proposed principles for model-based control of the microvia fill process are feasible.

5 Conclusions

At the time being, PCB manufacturing is already a high-volume, narrow-margin field of high-tech industry and the throughput volume as well as the output quality of the PCB production processes are continuously being improved in order to cut costs and to increase the efficiency of the manufacturing line. The complexity of the PCB production processes makes the experimental procedures for studying them lengthy and prone to mistakes. The utilization of detailed process models, which can swiftly deliver accurate and versatile information of the target process is, therefore, only due to increase in process design and optimization.

This thesis presents and discusses the components that are necessary for system-wide modeling of the microvia fill electroplating process as it is applied in PCB manufacturing. Aspects related to microscale phenomena, such as the additive effects on superconformal growth of the copper deposit, and to macroscale issues like cell design, voltage control and electrolyte ohmic loss, are discussed with respect to the computational modeling of these phenomena. A practical perspective to the subjects is kept throughout the whole work, which makes the further utilization of the presented models and methods more straightforward, than if the discussion was purely theoretical.

Two-dimensional surface growth models of the copper deposit during the microvia filling process were developed and described. The presented models were compared against measured via filling time-series data and detailed information of the parameters used in the numerically implemented models was given. The models were utilized to study what effects the chemical composition of the via fill bath and the thermodynamic properties of the components included in the bath have on the process output quality. The microvia fill models were also utilized in an extensive simulation-based study of two control strategies for the microvia fill process.

Two separate models were created to support the microvia fill process model development. One model was created for the model-based examination of the two-step copper redox reaction mechanism under the influence of multiple concurrent reactions. Another model was created to develop and investigate a model structure that enables incorporating all essential components of electric potential in an electrolysis cell system into one computational cell model. Both models were implemented computationally and parameterized, as well as validated by using experimental data. Additionally, a clarification of the computational techniques related to the FEM-ALE framework behind the microvia fill models was carried out and several estimators were developed to approximate various physical properties of the chemical species included in the models. All the models and computational tools developed within this work were implemented using commercial tools that are readily available

to everybody.

The work presented in this thesis covers all the aspects that need to be addressed when a system-wide model of the microvia fill process is developed. The work shows that implementing the theoretical models of the phenomena included in the microvia fill process system is possible and practically feasible. The thesis, therefore, provides several computational tools to any engineer working with the chemistry, the equipment or the process control of an industrial microvia fill process. It is suggested that by applying such tools and methods as discussed in this thesis, the utilization of the microvia interconnect technology will become more reliable, and more cost effective than it is now, even as the production conditions keep changing with an increasing pace.

References

[1] T. Närhi. Personal communication, 2009. Briefing held with T. Närhi (M.Sc.) of Meadville Aspocomp Intl. Ltd., at TKK, May 2009 and e-mail correspondence.

[2] A. Pohjoranta. *Modelling Surfactant Mass Balance on Deforming 2D Surfaces with the ALE Method*. 2008. Report 159, Helsinki University of Technology Control Engineering, ISBN 978-951-22-9931-7, http://lib.tkk.fi/Lic/2008/urn100088.pdf.

[3] Z. Wang, O. Yaegashi, H. Sakaue, T. Takahagi, and S. Shingubara. Bottom-up fill for submicrometer via holes of ulsis by electroplating. *Journal of the Electrochemical Society*, 151(12):C781–C785, 2004.

[4] COMSOL AB. *COMSOL Multiphysics User Guide and Model Library, version 3.5a, 3.5.0.606*. COMSOL AB, 2008. Sweden.

[5] MathWorks. *Matlab Release 14 with Service Pack 3 User Manual*. The MathWorks Inc., 2005.

[6] A.J. Pohjoranta. Microvia fill electroplating: a model for process monitoring development. Master's thesis, 2006. Master's thesis, Helsinki University of Technology, Control Engineering, http://users.tkk.fi/u/apohjora/pohjoranta_MSc_thesis_2006.pdf.

[7] IUPAC. *Compendium of Chemical Terminology, (the "Gold Book")*. Blackwell Scientific Publications, 2nd edition, 1997-2009. http://goldbook.iupac.org/.

[8] M. Paunovic and M. Schlesinger. *Fundamentals of Electrochemical Deposition*. John Wiley & Sons, 1998. ISBN 0-471-16820-3.

[9] M. Schlesinger and M. Paunovic. *Modern Electroplating*. John Wiley and Sons, 4th edition, 2000. ISBN 0-471-16824-6.

[10] R.S. Khandpur. *Printed Circuit Boards: Design, Fabrication and Assembly (eBook)*. McGraw-Hill, 2nd edition, 2005. ISBN 0-07-158925-2.

[11] J.F. Jr. Coombs. *Printed Circuits Handbook (eBook)*. McGraw-Hill, 6th edition, 2008. ISBN 0-07-151079-6.

[12] J. Newman and K.E. Thomas-Alyed. *Electrochemical Systems, 3rd edition*. John Wiley & Sons, 2004. ISBN 0-471-47756-7.

[13] A.J. Bard and L.R. Faulkner. *Electrochemical Methods; Fundamentals and Applications*. John Wiley & Sons, 2001. ISBN 0-471-043272-9.

[14] D. Pletcher and F.C. Walsh. *Industrial Electrochemistry*. Chapman and Hall, 2nd edition, 1990. ISBN 0-412-30410-4.

[15] C. Gabrielli, P. Mocoteguy, H. Perrot, A. Zdunek, and D. Nieto-Sanz. Influence of the anode on the degradation of the additives in the damascene process for copper deposition. *Journal of The Electrochemical Society*, 154(3):D163–D169, 2007.

[16] A.J. Cobley and D.R. Gabe. The effect of insoluble anodes on the process control and deposit quality of acid copper electroplating baths. *Circuit World*, 29(4):11–18, 2003.

[17] J.C. Lagarias, J.A. Reeds, M.H. Wright, and P.E. Wright. Convergence properties of the nelder-mead simplex algorithm in low dimensions. *SIAM Journal of Optimization*, 9(1):112–147, 1998.

[18] T. Kobayashi, J. Kawasaki, K. Mihara, and H. Honma. Via-filling using electroplating for build-up pcbs. *Electrochimica Acta*, 47:85–89, 2001.

[19] M. Lefebvre, G. Allardyce, M. Seita, H. Tsuchida, M. Kusaka, and S. Hayashi. Copper electroplating technology for microvia filling. *Circuit World*, 29(2):9–14, 2003.

[20] W-P. Dow and H-H. Cheng. A novel copper electroplating formula for laser-drilled micro via and through hole filling. *Circuit World*, 30(3):33–36, 2004.

[21] T. Närhi. Double microvia build-ups with viafilling technology. Master's thesis, 2005. Master's thesis, Tampere University of Technology, Department of Electrical Engineering.

[22] P.C. Andricacos, C. Uzoh, J.O. Dukovic, J. Horkans, and H. Deligianni. Damascene copper electroplating for chip interconnections. *IBM Journal of Research and Development*, 42(5):567–574, 1998.

[23] R. Akolkar and U. Landau. A time-dependent transport-kinetics model for additive interactions in copper interconnect metallization. *Journal of the Electrochemical Society*, 151(11):C702–C711, 2004.

[24] T.P. Moffat, D. Wheeler, and D. Josell. Superfilling and the curvature enhanced accelerator coverage mechanism. *The Electrochemical Society Interface*, 13(4):46–52, 2004.

[25] W.-P. Dow, M.-Y. Yen, C.-W. Liu, and C.-C. Huang. Enhancement of filling performance of a copper plating formula at low chloride concentration. *Electrochimica Acta*, 53:3610–3619, 2008.

[26] R. Akolkar and U. Landau. Mechanistic analysis of the "bottom-up" fill in copper interconnect metallization. *Journal of The Electrochemical Society*, 156(9):D351–D359, 2009.

[27] L. Bonou, M. Eyraud, R. Denoyel, and Y. Massiani. Influence of additives on cu electrodeposition mechanisms in acid solution: Direct current study supported by non-electrochemical measurements. *Electrochimica Acta*, 47:4139–4148, 2002.

[28] D.M. Soares, S. Wasle, K.G. Weil, and K. Doblhofer. Copper ion reduction catalyzed by chloride ions. *Journal of Electroanalytical Chemistry*, (532):353–358, 2002.

[29] M. Hayase, M. Taketani, K. Aizawa, T. Hatsuzawa, and K. Hayabusa. Copper bottom-up deposition by breakdown of PEG-Cl inhibition. *Electrochemical and Solid-State Letters*, 5(10):C98–C101, 2002.

[30] W-P. Dow and H-S. Huang. Roles of chloride ion in microvia filling by copper electrodeposition I. studies using sem and optical microscope. *Journal of The Electrochemical Society*, 152(2):C67–C76, 2005.

[31] W-P. Dow and H-S. Huang. Roles of chloride ion in microvia filling by copper electrodeposition II. studies using epr and galvanostatic measurements. *Journal of The Electrochemical Society*, 152(2):C77–C88, 2005.

[32] W-P. Dow, H-S. Huang, M-Y. Yen, and H-C. Huang. Influence of convection-dependent adsorption of additives on microvia filling by copper electroplating. *Journal of The Electrochemical Society*, 152(6):C425–C434, 2005.

[33] W-P. Dow, M-Y. Yen, W-B. Lin, and S.W. Ho. Influence of molecular weight of polyethylene glycol on microvia filling by copper electroplating. *Journal of The Electrochemical Society*, 152(11):C769–C775, 2005.

[34] T.P. Moffat, J.E. Bonevich, W.H. Huber, A. Stanishevsky, D.R. Kelly, G.R. Stafford, and D. Josell. Superconformal electrodeposition of copper in 500-90 nm features. *Journal of The Electrochemical Society*, l47(12):4524–4535, 2000.

[35] W-P. Dow, H-S. Huang, and Z. Linb. Interactions between brightener and chloride ions on copper electroplating for laser-drilled via-hole filling. *Electrochemical and Solid-State Letters*, 6(9):C134–C136, 2003.

[36] M. Tan and J.N. Harb. Additive behavior during copper electrodeposition in solutions containing Cl-, PEG, and SPS. *Journal of The Electrochemical Society*, 150(6):C420–C425, 2003.

[37] P.M. Vereecken, R.A. Binstead, H. Deligiani, and P.C. Andricacos. The chemistry of additives in damascene copper plating. *IBM Journal of Research and Development*, 49(1):3–18, 2005.

[38] M. Hayase, M. Taketani, T. Hatsuzawa, and K. Hayabusa. Preferential copper electrodeposition at submicrometer trenches by consumption of halide ion. *Electrochemical and Solid-State Letters*, 6(6):C92–C98, 2003.

[39] Z.V. Feng, X. Li, and A.A. Gewirth. Inhibition due to the interaction of polyethylene glycol, chloride, and copper in plating baths: A surface-enhanced raman study. *Journal of Physical Chemistry B*, 107(5):9415–9423, 2003.

[40] K.R. Hebert, S Adhikari, and J.E. Houser. Chemical mechanism of suppression of copper electrodeposition by poly(ethylene glycol). *Journal of the Electrochemical Society*, 152(5):C324–C329, 2005.

[41] K.R. Hebert. Role of chloride ions in suppression of copper electrodeposition by polyethylene glycol. *Journal of the Electrochemical Society*, 152(5):C283–C287, 2005.

[42] J. Mendez, R. Akolkar, and U. Landau. Polyether suppressors enabling copper metallization of high aspect ratio interconnects. *Journal of The Electrochemical Society*, 156(11):D474–D479, 2009.

[43] J.J. Kim, S-K. Kim, and Y.S. Kim. Catalytic behavior of 3-mercapto-1-propane sulfonic acid on cu electrodeposition and its effect on cu film properties for cmos device metallization. *Journal of Electroanalytical Chemistry*, 542:61–66, 2002.

[44] P. Taephaisitphongse, Y. Cao, and A.C. West. Electrochemical and fill studies of a multicomponent additive package for copper deposition. *Journal of The Electrochemical Society*, 148(7):C492–C497, 2001.

[45] T.P. Moffat, D. Wheeler, and D. Josell. Electrodeposition of copper in the SPS-PEG-Cl additive system: I. kinetic measurements: Influence of SPS. *Journal of The Electrochemical Society*, 151(4):C262–C271, 2004.

[46] K.C. Sung, S.-K. Kim, and J.J. Kim. Superconformal cu electrodeposition using DPS (a substitutive accelerator for bis(3-sulfopropyl) disulfide). *Journal of the Electrochemical Society*, 152(5):C330–C333, 2005.

[47] M. Tan, C. Guymon, D.R. Wheeler, and J.N. Harb. The role of SPS, MPSA and chloride in additive systems for copper electrodeposition. *Journal of the Electrochemical Society*, 154(2):D78–D81, 2007.

[48] D. Josell, D. Wheeler, W.H. Huber, and T.P. Moffat. Superconformal electrodeposition in submicron features. *Physical Review Letters*, 87(1):1–4, 2001.

[49] T.P. Moffat, D. Wheeler, W.H. Huber, and D. Josell. Superconformal electrodeposition of copper. *Electrochemical and Solid-State Letters*, 4(4):C26–C29, 2001. N.B. erratum.

[50] D. Wheeler, D. Josell, and T.P. Moffat. Modeling superconformal electrodeposition using the level set method. *Journal of the Electrochemical Society*, 150(5):C302–C310, 2003.

[51] W. Zhang, S.H. Brongersma, T. Conard, W. Wu, M. Van Hove, W. Vandervorst, and K. Maexa. Impurity incorporation during copper electrodeposition in the curvature-enhanced accelerator coverage regime. *Electrochemical and Solid-State Letters*, 8(7):C95–C97, 2005.

[52] Y. Cao, P. Taephaisitphongse, R. Chalupa, and A.C. West. Three-additive model of superfilling of copper. *Journal of The Electrochemical Society*, 148(7):C466–C472, 2001.

[53] S.-K. Kim, S. Hwang, K.C. Sung, and J.J. Kim. Leveling of superfilled damascene cu film using two-step electrodeposition. *Electrochemical and Solid-State Letters*, 9(2):C25–C28, 2006.

[54] K-C. Lin, J-M. Shieh, S-C. Chang, B-T. Dai, C-F. Chen, and M-S. Feng. Electroplating copper in sub-100 nm gaps by additives with low consumption and diffusion ability. *Journal of Vacuum Science and Technology B*, 20(3):940–945, 2002.

[55] S.-K. Kim, D. Josell, and T.P. Moffat. Electrodeposition of cu in the PEI-PEG-Cl-SPS additive system: Reduction of overfill bump formation during superfilling. *Journal of the Electrochemical Society*, 153(9):C616–C622, 2006.

[56] T.P. Moffat, D. Wheeler, S.K. Kim, and D. Josell. Curvature enhanced adsorbate coverage model for electrodeposition. *Journal of The Electrochemical Society*, 153(2):C127–C132, 2006.

[57] T.P. Moffat, D. Wheeler, S.-K. Kim, and D. Josell. Curvature enhanced adsorbate coverage mechanism for bottom-up superfilling and bump control in damascene processing. *Electrochimica Acta*, 53(1):145–154, 2007.

[58] H.A. Stone. A simple derivation of the time-dependent convective-diffusion equation for surfactant transport along a deforming interface. *Physics of Fluids A*, 2(1):111–112, 1990.

[59] G.K. Batchelor. *An Introduction to Fluid Dynamics*. Cambridge University Press, 1967. ISBN 789-0-521-66396-0.

[60] H. Wong, D. Rumschitzki, and C. Maldarelli. On the surfactant mass balance at a deforming fluid interface. *Physics of Fluids A*, 8(11):3203–3204, 1996.

[61] D. Josell, T.P. Moffat, and D. Wheeler. Superfilling when adsorbed accelerators are mobile. *Journal of The Electrochemical Society*, 154(4):D208–D214, 2007.

[62] G.S. Kim, T. Merchant, J. D'Urso, L.A. Gochberg, and Jensen K.F. Systematic study of surface chemistry and comprehensive two-dimensional tertiary current distribution model for copper electrochemical deposition. *Journal of the Electrochemical Society*, 153(11):C761–C772, 2006.

[63] C. West, S. Mayer, and J. Reid. A superfilling model that predicts bump formation. *Electrochemical and Solid-State Letters*, 4(7):C50–C53, 2001.

[64] M.J. Willey and A.C. West. A microfluidic device to measure electrode response to changes in electrolyte composition. *Electrochemical and Solid-State Letters*, 9(7):E17–E21, 2007.

[65] M.J. Willey and A.C. West. SPS adsorption and desorption during copper electrodeposition and its impact on PEG adsorption. *Journal of The Electrochemical Society*, 154(3):D156–D162, 2007.

[66] T.P. Moffat, D. Wheeler, M.D. Edelstein, and D. Josell. Superconformal film growth: Mechanism and quantification. *IBM Journal of Research and Development*, 49(1):19–36, 2005.

[67] M.L. Walker, L.J. Richter, and T.P. Moffat. Potential dependence of competitive adsorption of PEG, Cl^-, and SPS/MPS on cu (an in situ ellipsometric study). *Journal of The Electrochemical Society*, 154(5):D277–D282, 2007.

[68] Y-B. Li, W. Wang, and Y-L. Li. Adsorption behavior and related mechanism of janus green b during copper via-filling process. *Journal of The Electrochemical Society*, 156(4):D119–D124, 2009.

[69] M. Stangl, J. Acker, S. Oswald, M. Uhlemann, T. Gemming, S. Baunack, and K. Wetzig. Incorporation of sulfur, chlorine, and carbon into electroplated cu thin films. *Microelectronic Engineering*, (84):54–59, 2007.

[70] M. Kang and A.A. Gewirth. Influence of additives on copper electrodeposition on physical vapor deposited (PVD) copper substrates. *Journal of the Electrochemical Society*, 150(6):C426–C434, 2003.

[71] A. Frank and A.J. Bard. The decomposition of the sulfonate additive sulfopropyl sulfonate in acid copper electroplating chemistries. *Journal of The Electrochemical Society*, 150(4):C244–C250, 2003.

[72] C.-C. Hung, Lee W.-H., S.-Y. Hu, S.-C. Chang, K.-W. Chen, and Y.-L. Wang. Investigation of bis-(3-sodiumsulfopropyl disulfide) (SPS) decomposition in a copper-electroplating bath using mass spectrometry. *Journal of The Electrochemical Society*, 155(5):H329–H333, 2008.

[73] K. Doblhofer, S. Wasle, D.M. Soares, K.G. Weil, and G. Ertl. An eqcm study of the electrochemical copper(ii)/copper(i)/copper system in the presence of PEG and chloride ions. *Journal of the Electrochemical Society*, 150(10):C657–C664, 2003.

[74] D.R. Gabe and A.J. Cobley. Catalytic anodes for electrodeposition: a study for acid copper printed circuit board (pcb) production. *Circuit World*, 32(3):3–10, 2006.

[75] K.R. Hebert. Analysis of current-potential hysteresis during electrodeposition of copper with additives. *Journal of the Electrochemical Society*, 148(11):C726–C732, 2001.

[76] J.O. Dukovic. Feature-scale simulation of resist-patterned electrodeposition. *IBM Journal of Research and Development*, 37(2):125–142, 1993. ISSN 0018-8636.

[77] Y.H. Im, M.O. Bloomfield, S. Sen, and T.S. Cale. Modeling pattern density dependent bump formation in copper electrochemical deposition. *Electrochemical and Solid-State Letters*, 6(3):C42–C46, 2003.

[78] R. Akolkar and V. Dubin. Pattern density effect on the bottom-up fill during damascene copper electrodeposition; analysis of the suppressor concentration field effect. *Electrochemical and Solid-State Letters*, 10(6):D55–D59, 2007.

[79] Barkey D.P., Callahan J., Keigler A., Liu Z., Ruff A., Trezza J., and Wu B. Studies on through-chip via filling for wafer-level 3d packaging. 2006. 210th ECS Meeting, 2006, Abstract #1642.

[80] R.D. Braatz, R.C. Alkire, E. Rusli, and T.O. Drews. Multiscale systems engineering with applications to chemical reaction processes. *Chemical Engineering Science*, 59:5623–5628, 2004.

[81] R.D. Braatz, R.C. Alkire, E. Seebauer, E. Rusli, R. Gunawan, T.O. Drews, X. Li, and Y. He. Perspectives on the design and control of multiscale systems. *Journal of Process Control*, 16:193–204, 2004.

[82] T.J. Pricer, M.J. Kushner, and R.C. Alkire. Monte carlo simulation of the electrodeposition of copper: I. additive-free acid sulfate solution. *Journal of the Electrochemical Society*, 149(8):C396–C405, 2002.

[83] T.J. Pricer, M.J. Kushner, and R.C. Alkire. Monte carlo simulation of the electrodeposition of copper: II. acid sulfate solution with blocking additive. *Journal of the Electrochemical Society*, 149(8):C406–C412, 2002.

[84] Y. Kaneko, Y. Hiwatari, and K. Ohara. Monte carlo simulation of thin film growth with defect formation: Application to via filling. *Molecular Simulation*, 30(13):895–899, 2004.

[85] X. Li, T.O. Drews, E. Rusli, F. Xue, Y. He, R. Braatz, and R. Alkire. Effect of additives on shape evolution during electrodeposition: I. multiscale simulation with dynamically coupled kinetic monte carlo and moving-boundry finite-volume codes. *Journal of the Electrochemical Society*, 154(4):D230–D240, 2007. N.B. erratum.

[86] E. Rusli, F. Xue, T.O. Drews, P.M. Vereecken, P. Andricacos, Hariklia Deligianni, R.D. Braatz, and R.C. Alkire. Effect of additives on shape evolution

during electrodeposition: II. parameter estimation from roughness evolution experiments. *Journal of the Electrochemical Society*, 154(11):D584–D597, 2007.

[87] D. Adalsteinsson and J.A. Sethian. A level set approach to a unified model for etching, deposition, and lithography: I. algorithms and two-dimensional simulations. *Journal of Computational Physics*, 120:128–144, 1995.

[88] D. Adalsteinsson and J.A. Sethian. A level set approach to a unified model for etching, deposition, and lithography: II. three-dimensional simulations. *Journal of Computational Physics*, 122:348–366, 1995.

[89] Y. Kaneko. Personal communication, 2009. E-mail correspondence, May 2009.

[90] D. Josell, D. Wheeler, W.H. Huber, J.E. Bonevich, and T.P. Moffat. A simple equation for predicting superconformal electrodeposition in submicrometer trenches. *Journal of The Electrochemical Society*, 148(12):C767–C773, 2001.

[91] D. Josell, D. Wheeler, and T.P. Moffat. Superconformal electrodeposition in vias. *Electrochemical and Solid-State Letters*, 5(4):C49–C52, 2002.

[92] A.C. West. Theory of filling high-aspect ratio trenches and vias in presence of additives. *Journal of The Electrochemical Society*, 147(1):227–232, 2000.

[93] M. Georgiadou, D. Veyret, R.L. Sani, and R.C. Alkire. Simulation of shape evolution during electrodeposition of copper in the presence of additive. *Journal of The Electrochemical Society*, 148(1):C54–C58, 2001.

[94] M. Georgiadou and D. Veyretz. Modeling of transient electrochemical systems involving moving boundaries (parametric study of pulse and pulse-reverse plating of copper in trenches). *Journal of the Electrochemical Society*, 149(6):C324–C330, 2002.

[95] J. Bonet and R.D. Wood. *Nonlinear Continuum Mechanics for Finite Element Analysis*. Cambridge University Press, 1997. ISBN 0-521-57272-X.

[96] J. Donea and A. Huerta. *Finite Element Methods for Flow Problems*. Wiley, 2003. ISBN 0-417-49666-9.

[97] A.M. Winslow. Numerical solution of the quasilinear poisson equation in a nonuniform triangle mesh. *Journal of Computational Physics*, 135:128–138, 1997. reprinted, original version published 1966.

[98] E.M. Knobbe. A fem-ale approach for continuous domains with arbitrary moving boundaries. In *ECCOMAS 2004, Jyväskylä, Finland*, pages 1–20, 2004.

[99] H. Kardestuncer. *Finite Element Handbook*. McGraw-Hill, 1987. ISBN 0-07-033305-X.

[100] M.J. West, Q. Wang, and T.H. Bailey. Advanced metrology and control of copper electrochemical deposition I: The decomposition chemistry of the accelerator SPS. *Electrochemical Society Transactions*, 2(6):131–148, 2007.

[101] S.-K. Kim, D. Josell, and T.P. Moffat. Cationic surfactants for the control of overfill bumps in cu superfilling. *Journal of the Electrochemical Society*, 153(12):C826–C833, 2006.

[102] S.-K. Kim, D. Josell, and T.P. Moffat. Control of overfill bumps in damascene cu electrodeposition. *The Electrochemical Society Transactions*, 2(6):93–106, 2007.